Liposomal drug delivery in multimodal cancer therapy

Eirik Hagtvet

Dissertation for the degree of Philosophiae Doctor

Department of Radiation Biology
Institute for Cancer Research
Oslo University Hospital

Faculty of Medicine
University of Oslo

Series of dissertations submitted to the
Faculty of Medicine, University of Oslo
No. 1126

ISBN 978-82-8264-265-1

Cover: Inger Sandved Anfinsen.
Printed in Norway: AIT Oslo AS.

Produced in co-operation with Unipub.
The thesis is produced by Unipub merely in connection with the
thesis defence. Kindly direct all inquiries regarding the thesis to the copyright
holder or the unit which grants the doctorate.

Table of contents

Acknowledgements

The work presented in this thesis was carried out at the Department of Radiation Biology, Institute for Cancer Research, The Norwegian Radium Hospital, Oslo University Hospital, Oslo, Norway and Epitarget AS, Oslo, Norway between February 2008 and August 2011. Financial support was provided by the Norwegian Research Council, Epitarget AS and Radiumhospitalets Legater.

This work would not have been possible without the help and support of a large number of people.

I would like to express great gratitude to my supervisor Professor Dag Rune Olsen for giving me the possibility to write this PhD thesis in the exiting field of liposome research. His academic enthusiasm, positive attitude and commitment have been great motivational factors during the whole process.

Special thanks also go to my co-supervisor Dr. Esben A. Nilssen for always being positive, inspiring and helpful. In particular I have appreciated the generosity with which he always found time for discussions despite a busy work schedule.

My thanks further extend to Dr. Sigrid Fossheim, for helpful, motivating and valuable discussion. Also, thanks to Tove J. Evjen, Sibylla Røgnvaldsson and Andrew Fowler for manufacturing liposomes necessary for performing experiments, for fruitful discussions and for creating such a positive atmosphere at work!

Also, thanks to Kathrine Røe for introducing me to the field of MRI and for analyzing MRI data. I have also greatly appreciated the constructive discussions I have had with Tord Hompland concerning MRI experiments, with Alexandr Kristian regarding animal experiments and with Sebastian Patzke concerning fluorescence measurements.

Thanks also to Dr. Cyril Lafon's research group at INSERM, Lyon, France, for inspiring discussions and to Dr. Derek Tobin for proofreading parts of this thesis.

Finally, I would like to thank family and friends for continuous support through these years. In particular my mother and father for always motivating and encouraging me in this process.

Oslo, August 2011

Eirik Hagtvet

Abstract

Encapsulating cytostatics into lipid vesicles, i.e. liposomes, improves tumour drug accumulation and reduce adverse effects. Liposomal doxorubicin (DXR) has been used in the treatment of a variety of cancers and may also be suitable for combining with other treatment modalities. By modulating liposomal membranes, liposomes can be made ultrasound (US) sensitive releasing encapsulated drug in tumour tissue upon external US stimulation and may thereby improve therapeutic outcome. Moreover, as DXR is a potent radiosensitizer, liposomal DXR could enhance the effect of radiotherapy (RT) primarily in tumour tissue.

This thesis evaluates multimodal cancer therapy combining liposomal DXR with US and RT in tumour-bearing mice. Also, the feasibility of using *in vivo* fluorescence optical imaging (OI) to study liposome tumour uptake was evaluated. Enhanced therapeutic effect of liposomal DXR was observed when combined with US applied to tumour. Liposomal DXR also improved therapeutic outcome of RT under radioresistant hypoxic conditions. The role of OI in quantitative assessment of liposome tumour uptake remains unresolved.

Declaration of interest

Regarding publications included in this thesis; Tove J. Evjen, Sigrid L. Fossheim, Esben A. Nilssen and Sibylla Røgnvaldsson have ownership interests in Epitarget AS. Eirik Hagtvet and other co-authors have no such interests in Epitarget AS and report no conflict of interest.

Abbreviations

RT	Radiotherapy
PCa	Prostate cancer
PSA	Prostate specific antigen
ADT	Androgen depravation therapy
HIFU	High intensity focused ultrasound
PL	Phospholipid
DOPE	1,2 dioleoyl-sn-glycero-3-phosphatidylethanolamine
DSPE	1,2 distearoyl-sn-glycero-3-phosphatidylethanolamine
DSPC	1,2 distearoyl-sn-glycero-3-phosphatidylcholine
MPS	Monocyte phagocyte system
PEG	Polyethylene glycol
DXR	Doxorubicin
PL-DXR	Pegylated liposomal doxorubicin
US	Ultrasound
HFUS	High frequency ultrasound
LFUS	Low frequency ultrasound
CRT	Chemoradiotherapy
OI	Optical imaging
DiD	1,1'-dioctadectyl-3,3,3',3',-tetramethylindotricarbocyanine,4-chlorobenzenesulfonat salt
ROI	Region of Interest
DCE MRI	Dynamic contrast enhanced magnetic resonance imaging
RSI	Relative signal intensity
EES	Extracellular extravascular space
NIR	Near infrared
$AlPcS_4$	Al(III) Phthalocyanine Chloride Tetrasulfonic acid
HSPC	Hydrogenated-soy-phosphatidylcholine
PC	Phosphatidylcholine
PE	Phosphatidylethanolamine
FDA	Food and Drug Administration

1. Introduction

1.1 Cancer

Each year more than 12 million people are diagnosed with and 7.6 millions die from cancers worldwide. The cancers most commonly diagnosed are lung, breast and colorectal cancers while the most common causes of cancer deaths worldwide are cancers of lung, stomach and liver [1]. In Norway one in three will develop cancer by the age of 75 [2].

Cancer cells derive from normal cells. Normal cells however, divide at a controlled rate and participate in constructing a variety of tissues and functions. By contrast, cancer cells have an uncontrolled cell division and are less differentiated than healthy cells, lacking the ability to perform their intended functions [3].

Transformation from healthy to malignant tissue is a step-wise process where tissues of intermediate appearances can be identified. A modest deviation from healthy tissues are *hyperplastic* growths in which cells deviate only minimal in appearance but the numbers of cells are increased. An equally minimal deviation from healthy tissues is termed *metaplasia*, i.e. when one type of cell is displaced by an other cell type having normal appearance but not usually present at the location. A more abnormal growth is termed *dysplasia*. In this case the excessive numbers of cells also have abnormal appearances. All these growths are benign. However, if the transformation continues a malignant primary tumour may be the end product. Malignant tumours may grow invasively into neighbouring tissues and cancer cells may also spread by the bloodstream and lymphatic system forming metastases in sites far away from the primary tumour. Metastases are responsible for 90 % of deaths from cancer. Although there are exceptions, the transformation from healthy cells to cancer cells may progress over years or even decades. Most cancers are diagnosed at older age, indicating that tumour progression may be a long process. For a review see [3].

85 % of cancer cases involve solid tumours [4] characterized by a disorganized architecture with malfunctioning cells. Immature blood supply frequently fails to deliver oxygen and nutrients to rapidly dividing cells resulting in a tumour microenvironment characterized by

hypoxia and reduced pH. Reduced vascular functions represent a major obstacle for successful cancer treatment as therapeutic agents are not sufficiently delivered to less vascularised regions. Hypoxia also reduces the effect of treatment, i.e. radiotherapy (RT) and cytostatics. For a review see [5].

Causes of cancers may be numerous, i.e. genetics, physical and chemical carcinogens, lifestyles and infections [6]. However, as different cancers occur at very different frequencies between populations, numerous factors of both environmental and hereditary nature may participate in producing cancer [3].

Upon cancer diagnosis the most common treatment approach for solid tumours involve surgical removal of tumour tissue and if necessary followed by RT and/or chemotherapy. However, an increasing number of other therapeutic agents are also being used, e.g. immunotherapies and anti-angiogenic therapies [6].

1.2 Prostate cancer

The prostate gland is located at the neck of the bladder in males and contributes to the production of the seminal plasma. The glandular tissue is surrounded by a connective tissue capsule. Of the 26000 new cancer cases in Norway in 2008, 4200 were prostate cancer (PCa) making PCa the most common cancer among males in Norway [2]. PCa is classified clinically by the tumour size, lymph node involvement, and presence of metastasis according to the TNM-system (Table 1) [7] and histologically by the Gleason score [8]. Also, levels of prostate specific antigen (PSA) in the blood are used for diagnosis, deciding treatment strategy and treatment monitoring [9-11].

Tumour, node, metastasis (TNM) classification of PCa		
Primary tumour (T)	**Regional lymph nodes (N)**	**Distant metastasis (M)**
T0: No evidence of primary tumour	N0: No positive regional lymph node(s) metastasis	M0: No distant metastasis
T1: Clinically inapparent tumour neither palpable nor visible by imaging	N1: Metastasis in regional lymph node(s)	M1: Distant metastasis
T2: Tumour confined within prostate		
T3: Tumour expands through the prostate capsule		
T4: The tumour has invaded other nearby structures		

Table 1. TNM classification of PCa.

Treatment of PCa depends on the stage of the disease, whether the intention of treatment is curative or palliative as well as the patient's view on potential side effects. For curative treatment; surgery, external RT or brachytherapy, i.e. implantation of a radioactive source in the prostate, are being used. Further, external RT and brachytherapy or external RT and hormonal therapy, i.e. androgen deprivation therapy (ADT), may also be given in combinations [12]. Palliative treatments are commonly performed by administering combinations of ADT, surgery, RT and cytostatics. Taxanes is currently the cytostatics of choice [9,12]. Also, other innovative treatments such as high intensity focused ultrasound (HIFU) are being performed in localized and low or intermediate-risk PCa [13,14].

Radical prostatectomy is the only surgical technique performed with curative intentions. Other surgical procedures, like removal of metastases, are performed for palliative purposes. However, surgery involving the prostate may lead to significant side effects [12].

Radiation is administered both for curative and palliative intentions. It is either given by external RT or by brachiotherapy [12].

PCa arise as an “androgen-dependent” form, i.e. it is dependent of androgens to grow and consequently ADT may inhibit tumour growth for periods up to several years. However, ADT never cure PCa and after a remissive period the disease may enter an “androgen-independent” form where tumour growth occurs without the presence of androgens. Androgen-independent PCa does not respond to ADT [15].

PCa often develops slowly and may, especially in older patients, never progress into clinical PCa before the patients die of other reasons. Curative PCa treatment may involve serious side effects limiting quality of life. Therefore, several aspects have to be considered when deciding upon treatment. In patients with low risk of disease progression, *watchful waiting* may be employed, a strategy where treatment is actively postponed and the patient is routinely examined for progression of the disease [16]. Even though a variety of treatments are available, the numbers of deaths due to PCa are increasing [2] indicating that new treatment strategies are needed.

1.3 Liposomes

Liposomes are simple colloidal vesicles with an aqueous interior enclosed by a membrane usually composed of phospholipid (PL) molecules. PLs, the major components of biological membranes, are amphiphilic compounds with a polar head group and lipophilic acyl chains. PLs can be classified according to type of polar head group, fatty acid chain length and degree of saturation [17]. Figure 1 illustrates the structures of dioleoylphosphatidylethanolamine (DOPE), distearoylphosphatidylethanolamine (DSPE) and distearoylphosphatidylcholine (DSPC), which are PLs used in this thesis.

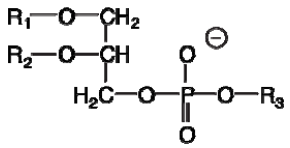

DOPE: R_1=R_2= C18:1, R_3= -$CH_2CH_2^{\oplus}NH_3$
DSPE: R_1=R_2= C18:0, R_3= -$CH_2CH_2^{\oplus}NH_3$
DSPC: R_1=R_2= C18:0, R_3= -$CH_2CH_2^{\oplus}N(CH_3)_3$

Figure 1. General structure of PLs and the structures of DOPE, DSPE and DSPC.

When bilayer forming PLs are dispersed in aqueous media they will spontaneously align themselves in a manner to reduce interactions between the polar media and the hydrophobic fatty acid chains. Consequently, bilayered structures, i.e. liposomes, may be formed. Liposomes may consist of one or more bilayers (lamellae) and of sizes ranging from tens of nanometres to tens of micrometers in diameter. For a review see [17]. Liposomes are broadly classified into small unilamellar vesicles (SUV; single bilayer, size 10 - 100 nm), large unilamellar vesicles (LUV; single bilayer, size 100 - 1000 nm), multilamellar vesicles (MLV, several bilayers, size 100 nm - 20 um and multivesicular vesicles (MVV, size 100 nm - 20 um) [18].

Since liposomes were first described 45 years ago [19] they have gained interests for a variety of applications including drug delivery [20]. Liposomes used for drug delivery are usually about 100 nm in size and are made up of a single bilayer. As liposomes comprise an aqueous core sealed of by a PL membrane both hydrophilic and lipophilic drugs can be accommodated in their respective compartments [18]. Today there are about 15 liposomal drugs approved for clinical applications or undergoing clinical evaluation [20]. Figure 2 presents a schematic illustration of drug encapsulated in a liposome.

Figure 2. Liposomal encapsulated drug. Epitarget©

1.4 Liposomes in cancer treatment

Conventional cytostatics used in cancer treatment are small molecular weight molecules [4]. Such molecules distribute non-specifically to both healthy and tumour tissue resulting in therapy limiting toxicities. To increase the therapeutic-to-toxicity ratio cytostatics can be encapsulated into small liposomes (~100 nm), which accumulate in tumours due to the

enhanced permeability and retention effect [21]. Here, leaky tumour vessels allow macromolecules to extravasate into tumour tissue, whilst reduced lymphatic tumour drainage results in particle accumulation.

First generation liposomes used for drug delivery suffered from fast clearance by cells of the monocyte phagocyte system (MPS). By coating liposomes with polyethylene glycol (PEG), i.e. pegylated liposomes, adhesion of plasma proteins and opsonins to liposomes are decreased. Consequently, immune system recognition is reduced, decreasing MPS uptake and prolongs circulation time [22]. Today, most liposomes used for drug delivery are pegylated.

1.5 Liposomal doxorubicin

The anthracycline anti-neoplastic drug doxorubicine (DXR) is active against a variety of tumours [23]. DXR is also very suitable for liposomal encapsulation due to the remote loading technique resulting in high drug-to-lipid levels [24]. Also, encapsulated DXR forms an insoluble gel contributing to stability [24]. Due to these unique properties liposomal DXR is on of the most studied liposomal drugs.

During cancer therapy involving conventional DXR, adverse effects on cardiac functions are commonly encountered. In contrast, by encapsulating DXR into pegylated liposomes, i.e. pegylated liposomal DXR (PL-DXR), accumulation in the heart is reduced, enabling the administration of greater drug doses [25,26]. The PL-DXR formulation Caelyx® has been used in the treatment of several solid tumours [22,24], including PCa [27-30] for which only a modest benefit was reported. However, these studies were performed with patients having progressed cancer, i.e. metastatic androgen-independent PCa, and the results may therefore not be clinically relevant for less advanced PCa.

1.6 Triggered drug release

Upon liposome tumour accumulation encapsulated drug has to become bioavailable prior to exerting cytotoxic actions [31]. Therapeutic effect of stable, long circulating liposomes may be hampered by decreased drug release in tumour tissue [24,32]. Finding methods to destabilize liposomes within tumour tissue are therefore nontrivial and could lead to

substantial increase in drug bioavailability with concurrent improved therapeutic outcome [24].

Several approaches have been proposed to induce drug release from liposomes including hyperthermia [33], enzymatic [34] and pH [35] mediated strategies. However, a growing line of evidence suggests that ultrasound (US) may enhance liposomal drug release improving therapeutic efficacy [36-38].

1.7 Ultrasound mediated drug delivery

US is defined as the transmission of pressure waves of frequencies above 20 kHz, which is the upper limit of human hearing [37]. US used in medical imaging employ frequencies between one and 20 MHz [39] delivered at low intensities (Watt/cm^2) [40]. In contrary, therapeutic US is generally delivered at medium and high intensities, and broadly classified according to frequency employed; low frequency US (LFUS), i.e. 20 - 100 kHz, and high frequency US (HFUS), i.e. 1 - 3 MHz [40]. Therapeutic US are used for a verity of purposes [40], including non-invasive HIFU treatment of PCa [14,41] and uterine fibroids [42]. Here, focused US of frequencies typically between 1 - 3 MHz are used to ablate tissues.

US can also be used for drug delivery purposes presumably due to acoustic cavitation, i.e. the oscillating movement of gas bubbles in a tissue exposed to US. A medium exposed to US will experience alternating intervals of high and low pressures. Under such conditions gas bubbles will expand at low pressures and contract at high pressures resulting in an oscillating movements of gas bubbles. When the oscillation is stable over several cycles it is termed *stable cavitation*. If, however, the US increases in magnitude the oscillating movements may result in collapse of gas bubbles, a process called *inertial cavitation*. During inertial cavitation neighbouring cell membranes or drug carrying vesicles can become transiently permeated, i.e. sonoporated [43,44]. Although not fully understood, cavitating gas bubbles in the vicinity of drug carriers are believed to be responsible for drug release. For reviews see [37,45,46].

In addition to inducing drug release from liposomes US may increase distribution of drugs in tumours, as well as increase cellular drug uptake [37]. US may also generate heat increasing extravasation of circulating drug carriers [47]. Consequently, US beneficial effects go beyond inducing drug release.

1.8 Sonosensitive liposomes

To render carrier molecules US-responsive the presence of air have traditionally been viewed necessary, e.g. liposomes containing air [48,49] and liposomes linked to microbubbles [50,51] have been developed. These structures are however, in micron scale and too large to extravasate prior to US treatment, limiting their use in cancer therapy. However, by changing membrane lipid composition, small liposomes (~100 nm) have been made US-responsive [52-54]. Such vesicles have the potential for both proper tumour accumulation and efficient drug release. Figure 3 illustrates a schematic representation of the treatment concept.

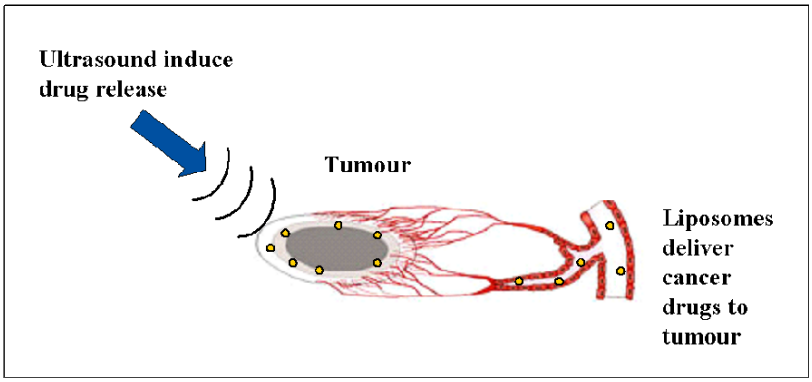

Figure 3. US mediated drug delivery from liposomes. Epitarget©

1.9 Liposomal doxorubicin in chemoradiotherapy

During tumour growth abnormal tumour vasculature frequently fails to supply sufficient levels of oxygen to tumour tissue, resulting in various degrees of hypoxia [55,56]. Tumour hypoxia is a well documented obstacle in achieving adequate response to RT as well as to other treatments including chemotherapy. Further, hypoxia is also known to promote malignant progression including metastatic development [57-59] and several strategies have been suggested to produce effective RT under hypoxic conditions [60,61].

Conventional cytostatics may also combine with RT, i.e. chemoradiotherapy (CRT), to enhance the effect or RT. Cytostatics may be used concurrent with RT, but also prior to, *neoadjuvant*, or after, *adjuvant*. Two such treatment modalities may interact positively and produce either *additive* or *synergistic* effects [62]. In strict sense a true “radiosensitizer”

should have no inherent cytotoxic activity [62]. However, the term is commonly used less strict and through this thesis it is used for any compound that enhances the effect of RT.

DXR is an efficient radiosensitizer [63-65] and by enclosing DXR into liposomes, drug distribution to tumours may be enhanced. Consequently, radiation sensitization may primarily be located to tumour tissue, reducing toxicities in neighbouring healthy tissues where less sensitizing drug would have accumulated [66,67]. Both PL-DXR [66,68] and non-pegylated liposomal DXR [69] have reportedly increased the effect of RT in animal models. Also, promising results have been obtained from smaller clinical studies [67,70].

2. Aim of thesis

This overall aims of this thesis were to investigating the potential therapeutic benefits of combining PL-DXR with other treatment modalities, i.e. US and RT, in preclinical models. Also, assessing the feasibility of using small animal fluorescence imaging, i.e. optical imaging (OI), during the development of liposomal formulations. The specific aims were to:

• Determine if the presence of DSPE in the liposomal membrane may render liposomes both US-responsive and stable in the blood stream.

• Assess if LFUS treatment can enhance the therapeutic outcome of DSPE-based liposomal DXR in mice bearing prostate cancer xenografts.

• Investigate how different levels of DOPE in the liposomal membrane influence US-sensitivity and stability *in vivo*.

• Examine if liposome labelling with the carbocyanine lipophilic tracer 1,1'-dioctadectyl-3,3,3',3',-tetramethylindotricarbocyanine,4-chlorobenzenesulfonat salt (DiD) is a suitable labelling technique for *in vivo* applications.

• Investigate if OI is a suitable imaging modality for studying biodistribution of fluorochrome labelled liposomes.

• Assess the impact of PL-DXR on vascular functions in prostate tumour xenografts.

• Examine if therapeutic effect of RT on hypoxic prostate xenografts may be enhanced by the co-administration of PL-DXR.

3. Materials and methods

3.1 Animals

Male atymic nude Balb/c mice were provided by the Department of Comparative Medicine, Radium Hospital, Oslo University Hospital, Oslo, Norway. The mice were housed in transparent boxes with bedding material, fed *ad libitum* and kept under specific pathogen-free conditions. The temperature and relative humidity were kept constant at 20 – 21 °C and 60 %, respectively. At the end of the experiments all animals were euthanized by cervical dislocation. All procedures were performed according to protocols approved by the National Animal Research Authority and carried out in compliance with the European Convention for the Protection of Vertebrates Used for Scientific Purposes. The animals were 4 - 6 weeks old at time of tumour implantation (Paper I, III, IV and section 5.1 and 5.2).

3.2 Tumour models

CWR22 human androgen dependent prostate adenocarcinoma, initially obtained from patients during surgery [71], were serially transplanted between mice. By blunt dissection through a skin incision above the caudal spine, a tumour fragment (~2x2x2 mm) was subcutaneously implanted on the flank (Paper I and section 5.2) or on the upper leg (Paper IV and section 5.1). The skin incision was sealed with topical skin adhesive.

22R*v1* human prostate adenocarcinoma (American Type Culture Collection, Manassas, VA, USA) is a cell line derived from CWR22 [72]. Cells were cultured in RPMI 1640 containing L-glutamine and $NaHCO_3$ (Sigma Aldrich, Oslo, Norway) supplemented with 10 % foetal bovine serum (Fisher Scientific, Oslo, Norway) and 100 units/ml + 0,1 mg/ml of Penicillin-Streptomycin (Sigma Aldrich, Oslo, Norway) at 37 °C in air containing 5 % CO_2. 10^6 tumour cells suspended in 50 µl supplement free growth medium was mixed 1:1 (v:v) with Matrigel® (VWR Oslo, Norway) and injected subcutaneously on the leg of mice and left to grow for 2-3 weeks until start of experiment (Paper III and section 5.1).

LEW2AX human liposarcoma, initially obtained from patients during surgery, were serially implanted in nude mice to generate subcutaneous xenografts (section 5.2). LEW2AX grows slower and more homogenous than the prostate models also used in this thesis.

3.3 Anaesthetics

For anaesthesia of mice, a mixture of 2.4 mg/ml tiletamine and 2.4 mg/ml zolazepam (Zoletil® vet, Virbac Laboratories, Carros, France), 3.8 mg/ml xylazine (Narcoxyl® vet, Roche, Basel, Switzerland) and 0.1 mg/ml butorphanol (Torbugesic®, Fort Dodge Laboratories, Fort Dodge, IA, USA) in sterile water was prepared and used. The dosage used was 0.05-0.1 ml/animal (Paper I, II, III and IV, section 5.1 and 5.2).

3.4 Ultrasound

In vivo US treatment (Paper I) was performed with a 40 kHz ultrasonic processor (Model VC 754, Sonic and Materials Inc., Newtown, CT, US) with a 19 mm diameter probe partially submerged into a cylinder containing deionized water, degassed by boiling, and cooled in ice bath. The bottom of the cylinder was sealed with a latex membrane in firm contact with the skin covering the tumour of an anesthetized mouse located on an adjustable plate. A thin layer of US gel was placed between the skin and the latex membrane. The US probe was run for a duration of four minutes and with a two cm distance between the probe and the skin.

In vivo US treatment (section 5.1) was performed with a focused 1.13 MHz confocal, i.e. two US transducers, setup developed at Dr. Cyril Lafon's lab, INSERM, Lyon, France. In brief, a tumour-bearing mouse was located on an adjustable plate with the xenograft facing upwards in firm contact with a latex membrane supported by a grid, creating a degassed water reservoir. The two US transducers and an imaging US probe were anchored to a metal rack (Figure 4). The metal rack was submerged into the water reservoir and positioned so that the cavitation zone was between the skin surface and the centre of the tumour. The correct positioning of the cavitation zone was assured by the US imaging probe. US treatment was performed for one minute with the animals under anaesthesia.

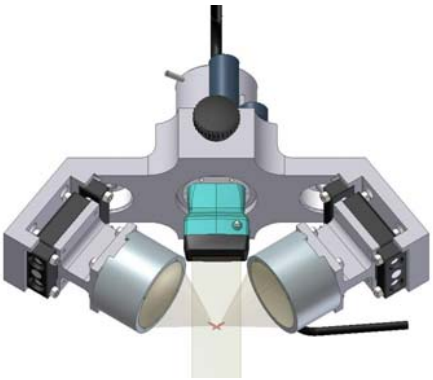

Figure 4. The two US transducers were anchored to a metal rack having identical focal spots. The presence of an imaging US probe ensured proper positioning of the cavitation zone within the tumour xenograft. INSERM©

In vivo US treatment (section 5.2) was performed using a 250 kHz focused US transducer (Model H115, Sonic Concepts, Bothell, WA, USA) connected to a cone shaped water chamber (C103 polycarbonate coupling cone for Model H115, Sonic Concepts, Bothell, WA, USA). A mouse bearing a tumour xenograft on the flank was located on an adjustable plate with an opening for the xenograft to be exposed downwards. The exposed xenograft was partially submerged into the water chamber containing degassed water that had been cooled in ice bath. US treatment was performed for five minutes with the mouse under anaesthesia.

3.5 *In vivo* fluorescence optical imaging

In vivo fluorescence imaging was performed with an IVIS® Imaging System 100 Series with XFO-6 Fluorescence Option (Xenogen corp., Alameda, CA, USA) (Paper III and section 5.1). All images were acquired using a Cy5.5 excitation filter (wavelength 615 - 665 nm), Cy5.5 background excitation filter (wavelength 580 - 610 nm) and Cy5.5 emission filter (wavelength 695 - 770 nm). Imaging data analysis was performed with Living Image® 2.5 software (Xenogen corp., Alameda, CA, USA) by subtracting the fluorescence background for each acquisition. Quantitative data for tumour fluorescence was obtained by manually drawing a region of interest (ROI) around the tumours visible margins. Average counts (sum of all counts inside ROI/no of pixels in ROI) were used during data interpretation. Prior to imaging,

the mice were sedated with 0.05 ml of anaesthetic agent sc. Figure 5 presents a representative image of tumour-bearing mice administered DiD labelled liposomes.

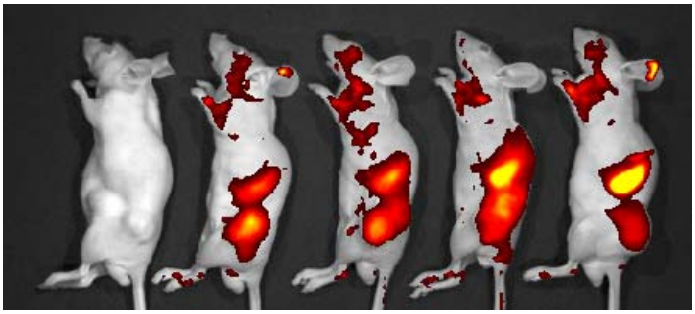

Figure 5: *In vivo* fluorescence imaging. Mice bearing 22R*v1* prostate tumour xenografts administered DiD-labelled liposomes. Fluorescence intensity is highest in tumour and liver regions. The mouse to the left is untreated.

3.6 Radiotherapy

Mice bearing xenogtafts were irradiated using ^{60}Co source (Mobaltron 80, TEM instruments, Crawley, UK) with a dose rate of 0.8 Gy/min. Each mouse were located in a custom designed vicryl tube containing an opening for the tumour-bearing leg to be stretched out and fixated horizontally. During the procedure only the tumour-bearing leg extended into the radiation field. The procedure was performed under sedation induced by 0.05 ml of anaesthetic agent (Paper IV).

3.7 Dynamic contrast enhanced magnetic resonance imaging

MRI acquisitions were performed as previously described [73], using a 1.5 T GE Signa LS scanner (GE Medical Systems, Milwaukee, WI), and a dedicated MRI mouse coil [74]. Prior to MRI, a heparinized 24 G catheter attached to a cannula containing 0.01 ml/g body weight of the contrast agent Dotarem® (Laboratoire Guerbet, Paris, France) diluted in heparinized saline to 0.06 M, was inserted into the animals' tail vein. The animals were placed in an adapted cradle and put into the mouse coil, before being placed in the scanner. During image acquisition, the animal's temperature was maintained at 38 °C. Dynamic contrast enhanced magnetic resonance imaging (DCE MRI) were performed by acquiring 5 baseline T1-

weighted image acquisitions followed by contrast injection over a period of three seconds. Contrast kinetics was investigated by 20 minutes of post-contrast imaging. Figure 6 presents T1-weighted images of a mouse bearing prostate xenografts.

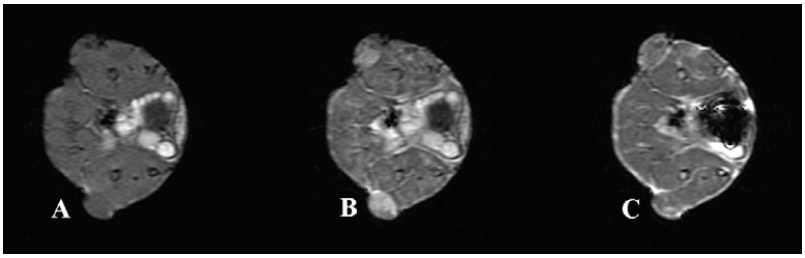

Figure 6. Cross section T1-weighted images of a mouse bearing two CWR22 prostate xenografts. Varying xenograft signal intensities can be observed: A; pre, B; 1 minute post and C; 20 minutes post iv administration of Dotarem®.

Image analysis was performed using in-house developed software in IDL (Interactive Data Language v 6.2, Research Systems Inc., Boulder, CO). For the central slice of each tumour, a ROI was manually drawn in the T1-weighted images, excluding surrounding skin and connective tissue. The time-dependent relative signal intensity, *RSI(t)*, was calculated for each image voxel according to Equation 1.

Equation 1: $$RSI(t) = \frac{SI(t) - SI(0)}{SI(0)}$$

where *SI(0)* refers to the pre-contrast signal intensity and *SI(t)* the post-contrast signal intensity in the voxel at time *t*.

Pharmacokinetic modelling was performed using the Brix model [75]. The Brix model is a two-compartment pharmacokinetic model where the contrast agent is assumed to distribute between two individually well-mixed compartments; the blood plasma and the extracellular extravascular space (EES) in the tumour. The iv injected contrast agent is transported into the tumour by perfusion, where it diffuses between the plasma and the EES, before being eliminated at a constant rate. Using the *RSI(t)* for each voxel in the tumor ROI, the Brix model

(Equation 2) was fitted using the Levenberg-Marquardt least-squares minimization method (MPFIT; http://purl.com/net/mpfit) [76].

Equation 2: $$RSI(t) = \frac{Ak_{ep}}{k_{el}k_{ep}}(e^{-k_{ep}t} - e^{-k_{el}t})$$

where the parameter k_{ep} is the rate constant between plasma and EES, k_{el} the clearance rate of contrast agent from plasma, and A an amplitude parameter related to the size of the EES [77] (Paper IV). Figure 7 portrays tumour uptake and elimination of Dotarem® in a CWR22 prostate xenograft.

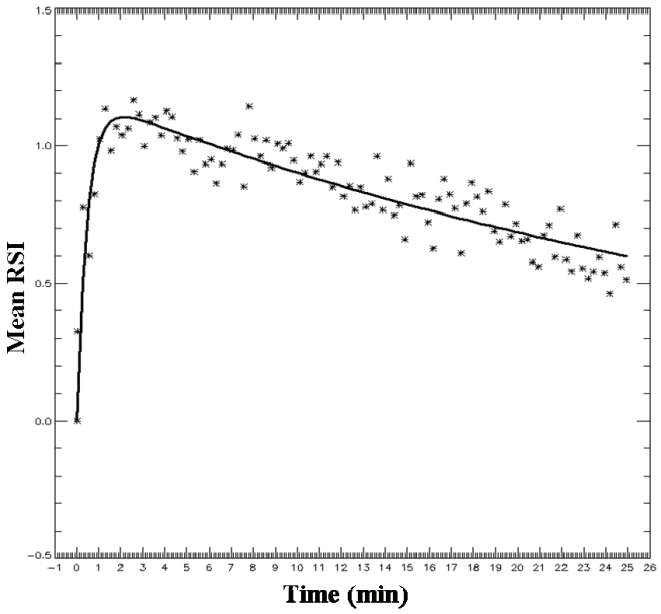

Figure 7. Mean *RSI(t)* from all voxels in a tumour ROI. The Brix model was fitted using the Levenberg-Marquardt least-squares minimization method. The plot illustrates a characteristic rapid tumour contrast uptake followed by gradual elimination from the tumour.

3.8 Immunohistochemistry

Hypoxia was determined by injecting 80 mg/kg pimonidazole hydrochloride (1-[(2-hydroxy-3-piperidinyl)propyl]-2-nitroimidazole hydrochloride (Natural Pharmacia International, Inc.,

Burlington, MA, USA), dissolved in saline, ip to tumour-bearing mice. One hour later euthanasia was performed by cervical dislocation and tumours were excised and preserved in phosphate-buffered 4 % formalin until tissue sectioning. Tumour hypoxia was detected using a peroxidase-based immunostaining method. In brief, tissue sections were stained using the Dako EnVision™+ System-HRP (DAB) (K4011) and Dakoautostainer. Deparaffinization and unmasking of epitopes were performed using PT-Link (DAKO) and EnVision™ Flex target retrieval solution, high pH. To block endogenous peroxidase, sections were treated with 0.03 % hydrogen peroxide for 5 min. The preparations were incubated 30 minutes with polyclonal rabbit antibodies to pimonidazole-protein adducts (1:10000 dilution). The sections were then incubated with peroxidase labeled polymer conjugated to goat anti-rabbit secondary antibodies for 30 minutes. Tissue was stained for 10 minutes with 3'3-diaminobenzidine tetrachloride (DAB) and counterstained with haematoxylin, dehydrated and mounted, and mounted in Diatex (Paper IV).

4. Summary of publications

Paper I

Ultrasound enhanced antitumour activity of liposomal doxorubicin in mice

***Eirik Hagtvet**, Tove J. Evjen, Dag Rune Olsen, Sigrid L. Fossheim, Esben A. Nilssen*

Journal of Drug Targeting, published

DSPE-based liposomes were evaluated as a potential US-sensitive delivery vehicle for DXR. *In vitro* characterization demonstrated 20 % DXR release from liposomes after four minutes of LFUS exposure in addition to high stability in serum assay. The biodistribution profile of the formulation was investigated by administering a drug dose of 3.5 mg DXR/kg to mice bearing prostate tumour xenografts. Approx 10 % of administered drug dose was accounted for in the blood 24 hours post injection indicating acceptable circulation time. High levels of DXR were also detected in liver and spleen. Tumour drug uptake reached plateau levels around 24 hours post injection.

Therapeutic effect was assessed by administering a drug dose of 3.5 mg DXR/kg to tumour-bearing mice. LFUS was delivered to the tumour 24 hours post injection by a 40 kHz US setup for a duration of four minutes. Therapeutic response was evaluated by tumour size measurements for 22 days. Neither DSPE-based liposomal DXR nor LFUS produced any growth inhibiting effect. However, DSPE-based liposomal DXR in combination with LFUS produced a significant reduction in tumour growth compared to the group administered only DSPE-based liposomal DXR.

Levels of dissolved gases, viscosity, plasma proteins etc. might affect drug release and clearly varied between *in vitro* and *in vivo* experiments in current study. It can therefore not be concluded that similar drug release levels were achieved both *in vitro* and *in vivo*. It renders that the observed tumour growth inhibition might also result from other effects induced by LFUS, such as enhanced cellular drug uptake and improved liposomal extravasation.

Nevertheless, the study demonstrates that LFUS may enhance the effect of DSPE-based liposomal DXR.

Paper II

Sonosensitive dioleoylphosphatidylethanolamine-containing liposomes with prolonged blood circulation time of doxorubicin

Tove J. Evjen, ***Eirik Hagtvet****, Esben A. Nilssen, Martin Brandl, Sigrid L. Fossheim*

European Journal of Pharmaceutical Sciences, published

DOPE-based liposomes were evaluated as potential US-sensitive delivery vehicles for DXR. Liposome formulations containing DOPE levels between 12 and 62 mol % were evaluated for *in vitro* US-sensitivity by using a 40 kHz US setup. US sensitivity increased with increasing DOPE content, i.e. the formulations comprising 12 and 62 mol % DOPE experienced a drug release of 11 % and 91 % respectively. For liposomes to sufficiently accumulate in tumour tissues a prolonged circulation time is considered necessary. Hence, the kinetic profiles of the formulations were investigated by administering a drug dose of 7 mg DXR/kg to mice. The formulations with the highest DOPE content, i.e. 52 and 62 mol % experienced a fast DXR clearance. In contrary, the formulations containing 25 and 32 mol % had a kinetic profile similar to Caelyx®, with approximately 20 % of the administered DXR dose accounted for in the bloodstream 24 hours after iv injection. DXR content in liver and spleen indicated that the faster blood clearance for DOPE-rich formulations was not the result of enhanced uptake by MPS but due to increased leakage of DXR from the liposome carriers. It should not be excluded however, that the different blood clearance of liposomes comprising different DOPE levels could be due to accumulation in tissues not investigated in the study, such as the skin or paws.

The reduction in liposomal DOPE content to 25 and 32 mol % did not significantly reduce US mediated DXR release *in vitro*, indicating that DOPE is a potent modulator of sonosensitivity. The study suggested that by modulating the liposomal membrane it is possible to combine high US-sensitivity with prolonged circulation time.

Paper III

Assessment of liposome biodistribution by non-invasive optical imaging: A feasibility study in tumour-bearing mice

Eirik Hagtvet*, Tove J. Evjen, Esben A. Nilssen, Dag Rune Olsen*

Journal of Nanoscience and Nanotechnology, submitted

The study evaluated the feasibility of using OI to study liposome accumulation in tumours. PL-DXR (Caelyx®) was labelled with DiD, a lipophilic carbocyanine tracer commonly used to label cells and liposomes for *in vivo* applications. No change in liposome size or serum stability was observed after the labelling procedure. Also, all administered dye appeared to be liposome associated *in vitro*.

The labelled liposomes were administered to mice bearing prostate xenografts at a dose of 14 mg DXR/kg iv. Subsequently, the *in vivo* distribution of the labelled liposomes was followed over time by OI acquisitions. The results revealed a gradual increase in tumour fluorescence, indicating accumulation of the liposomes reaching plateau levels at 48 hours post injection.

Parallel groups of animals were imaged at 24 or 48 hours post injection followed by sacrifice and tissue quantification of DXR and DiD. Blood sample analysis revealed that DiD levels where lower than DXR levels at both 24 and 48 hours indicating a faster elimination of DiD than DXR from the blood. The different elimination rates strongly suggest that DiD dissociated from liposomes *in vivo*. A similar scenario was seen in tumour tissue were more DXR than DiD were accounted for. This finding could presumably be explained by the dissociation of DiD from liposomes within the blood circulation resulting in more DXR than DiD being transported to tumour. Moreover, if DiD dissociated from liposomes in the circulation it will presumably, due to its highly lipophilic nature, associate with lipoproteins and other blood components leading to liver uptake. This may explain the significantly higher DiD levels in liver compared to DXR at both 24 and 48 hours post injection.

The fact that DiD seemingly dissociated from liposomes during circulation questions the suitability of DiD as a quantitative marker for liposomes *in vivo*. The results also indicate that *in vivo* cell application of carbocyanine dyes may have limitations.

In vivo measured fluorescence intensity correlated only weakly (R^2=0.59) with actual tumour DiD levels indicating that substantial scattering and absorption of *in vivo* fluorescent signal rendered it difficult to obtain reliable quantitative correlations between the biodistribution profile of the labelled liposomes.

Paper IV

Liposomal doxorubicin improves radiotherapy response in hypoxic prostate cancer xenografts

***Eirik Hagtvet**, Kathrine Røe, Dag Rune Olsen*

Radiation Oncology, submitted

Tumor hypoxia prevents effective RT and several strategies have been suggested to increase the effect of RT under hypoxic conditions. As DXR is known to enhance the effect of RT the current study examines the therapeutic benefit of combining PL-DXR (Caelyx®) with RT on radioresistant hypoxic tumours. PL-DXR was administered to mice bearing prostate carcinoma xenografts in combination with RT, both under normoxia and hypoxia, the latter being induced by clamping the tumour-bearing leg prior to and during RT. Treatment was assessed by tumour volume measurements for 29 days. RT alone had a profound antitumor effect, and literary stopped tumour growth. However, the effect of RT was significantly reduced when performed under hypoxic conditions. Moreover, concomitant administration of PL-DXR at a dose of 3.5 mg/kg significantly improved the therapeutic outcome of RT in hypoxic tumours.

To assess therapy mediated changes to tumour vascular functions DCE MRI with subsequent pharmacokinetic analysis, was performed pre-treatment (baseline) and 8 days later. Further, parallel groups of animals were used to assess hypoxic fractions by immunohistochemistry of excised tumour tissue. The pharmacokinetic DCE MRI parameters and hypoxic fractions

suggested PL-DXR to induce tumour growth-inhibitory effects without interfering with tumour vascular functions. This feature is highly beneficial with respect to concomitant RT since well vascularised tumours may be more oxygenated and more likely respond better to RT. Moreover, PL-DXR appeared to reduce some of the vascular damaging effects produced by RT under hypoxic conditions.

5. Brief presentation of non-published studies involving DOPE-based liposomes

Incorporating DOPE in the liposomal membrane may be a promising approach for rendering liposomes US-responsive. This section presents in brief two animal studies performed with DOPE-based liposomes. The studies are not included in any publications.

5.1 *In vivo* liposome sonosensitivity evaluated by optical imaging

When fluorochromes are encapsulated in high concentrations within liposomes the fluorescence signal emitted will be reduced, i.e. quenched [78,79]. Upon release of encapsulated substances fluorescence signal will increase and US mediated drug release may therefore be visualized by OI.

To evaluate liposome sonosensitivity *in vivo*, liposomes encapsulating the near infrared (NIR) fluorochrome, Al(III) Phthalocyanine Chloride Tetrasulfonic acid ($AlPcS_4$) [80] were produced. Two $AlPcS_4$-liposome formulations were prepared; sonosensitive DOPE-based liposomes (DOPE:DSPC:DSPE-PEG 2000:Cholesterol 25:27:8:40 mol %) and non-sonosensitive hydrogenated-soy-phosphatidylcholine (HSPC)-based liposomes (HSPC:DSPE-PEG 2000:Cholesterol 57:5:38 mol %), the latter having the same membrane composition as Caelyx® [81].

10 µl liposome dispersion was injected directly into 22R*v1* prostate tumour xenografts implanted on the leg of nude mice. Fluorescent images were acquired pre and post tumour exposure to 1.13 MHz US for 1 min using a confocal US setup developed at INSERM, Lyon, France.

Figure 8 and 9 presents representative images of animals administered HSPC-based liposomes and DOPE-based liposomes, respectively. Tumour signal intensity was quantified by drawing a ROI around the tumour. The group receiving DOPE-based liposomes combined with US experienced a significant increase in signal intensity (110%, $p<0.05$). The group receiving HSPC-based liposomes and US did not experience a significant increase. Neither

did control animals, i.e. animals receiving no US between the two image acquisitions. The mean group relative increases in fluorescence signal for the different experimental groups are presented in Figure 10.

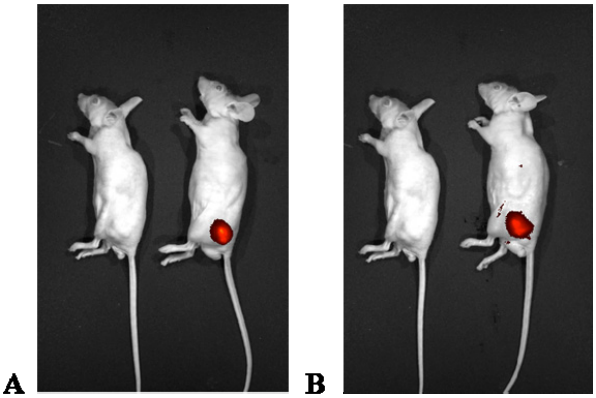

Figure 8. Mouse administered intratumoral injection of $AlPcS_4$-containing HSPC-based liposomes pre (A) and post (B) US treatment. The left animal is untreated control.

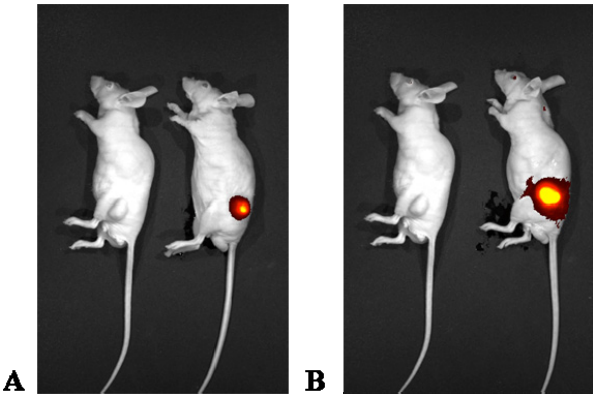

Figure 9. Mouse administered intratumoral injection of $AlPcS_4$-containing DOPE-based liposomes pre (A) and post (B) US treatment. The left animal is untreated control.

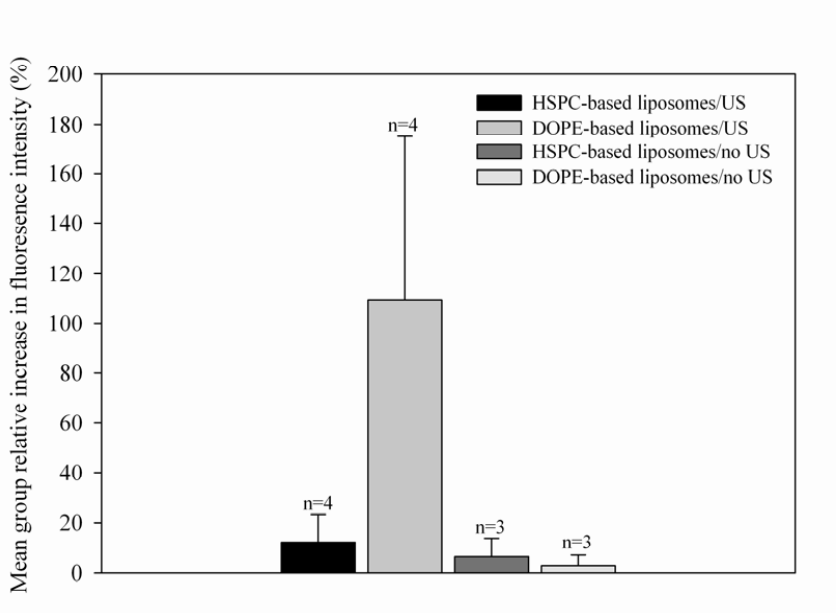

Figure 10. Mean group relative increase in fluorescence intensity. Group size and standard deviations are given.

It should be added that iv administration of $AlPcS_4$-containing DOPE-based liposomes with concurrent US treatment 5 or 24 hours later did not result in an increase in fluorescence intensity. This may be due to leakage in circulation, low tumour uptake, low assay sensitivity at lower concentrations or other reasons. It should also be emphasized that the current study included only a small number of animals. Firm conclusions may therefore not be made regarding *in vivo* sonosensitivity of current formulations. Nevertheless, the study provide support that US may induce drug release from liposomes *in vivo*.

5.2 Therapy study with DOPE-based liposomes

Sonosensitive DXR containing DOPE-based liposomes (DOPE:DSPC:DSPE-PEG 2000:Cholesterol 25:27:8:40 mol %), having identical membrane composition as DOPE-based liposomes described in section 5.1 were administered as a single iv injection to mice bearing LEW2AX liposarcoma xenografts. The LEW2AX xenograft model was used since it grows more homogenously than the prostate xenografts used elsewhere in this thesis. A relatively high drug dosage of 14 mg DXR/kg was administered iv and US treatment was

performed 24 hours later by a focused 250 kHz setup for a duration of five minutes. US treatment alone did not produce any tumour growth inhibition in animals receiving saline. Neither did US enhance tumour growth inhibition in animals administered DOPE-based liposomal DXR (Figure 11).

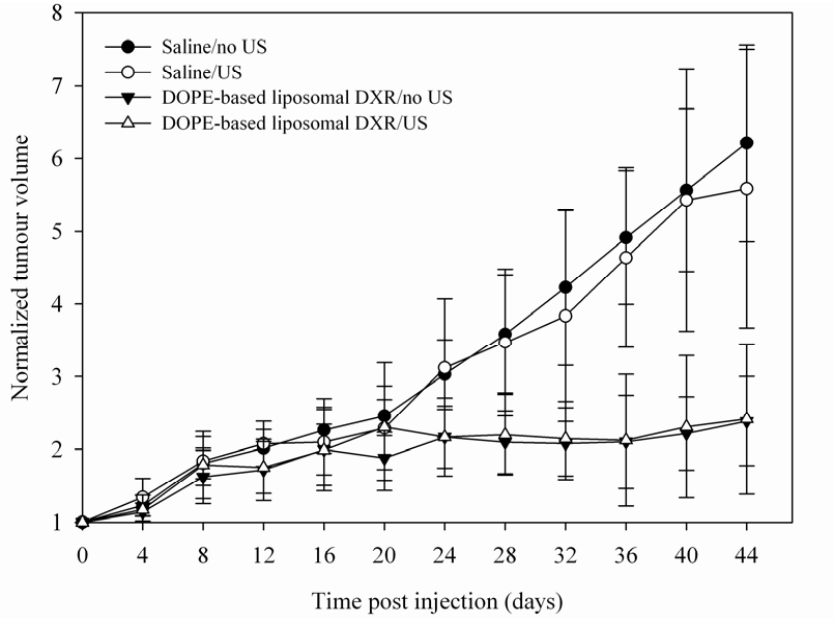

Figure 11. Tumour growth in mice. Group mean and standard deviations are given (n = 7 - 8).

Paper II demonstrated that the current DOPE-based liposomes administered were highly sonosensitive *in vitro* as well as exhibiting prolonged circulation time, i.e. 17 % of administered drug were present in the blood 24 hours post injection. Consequently, it could presumably be anticipated that US would enhance the therapeutic effect of DOPE-based liposomal DXR. However, US did not have any enhancing effect. Numerous reasons may explain the absence of such effect including low US-sensitivity of liposomes *in vivo*, failure of US setup to deliver sufficient intensity *in vivo* or other reasons. However, the relatively high dose of liposomal DXR alone literary ceased tumour growth reaching therapy saturation levels. In retrospect, if US produced any additional effect it is unlikely that it could have been identified. Consequently, the study might illustrate that when assessing therapeutic response

in dual therapy modalities, administering excessive amounts of one agent renders it difficult to observed combined effects.

6. Discussion

The ability of liposomes to transport therapeutic agents to tumour tissue may render liposomes an interesting drug delivery strategy for combining with other treatment modalities. By modulating the liposomal membrane composition, liposomes can be given special features like sonosensitivity. DXR have been used for treating several cancers and is also well suited for encapsulation into liposomes. Further, as DXR is a potent radiosensitizer liposomal DXR may be feasible to combine with RT.

In this thesis preclinical evaluations of dual therapy combining liposomal DXR with US and RT have been assessed in immunocompromised mice bearing human tumour xenografts. Subcutaneous tumour xenografts differ in many aspects from clinical tumours, e.g. they grow in anatomically inappropriate sites, rarely metastasize and grow very rapidly following implantation. The ability of tumour xenografts to predict clinical efficacy is therefore somewhat disputed. However, all therapeutic agents used for treating cancers clinically have also demonstrated activity in preclinical models [82].

6.1 Preclinical evaluation of sonosensitive liposomes

Tumour accumulation of liposomes is a slow process requiring prolonged circulation time to enable sufficient uptake in tumour tissue [24]. Consequently, liposome research has for the last decades focused on developing liposomes that minimize MPS recognition in addition to being stable in the blood stream so that any pre-emptive drug leakage prior to tumour extravasation is reduced. However, upon tumour accumulation encapsulated drug has to become bioavailable prior to exerting cytotoxic actions [31]. Liposomal drug release for stable, long circulating liposomes like Caelyx® is a long process and several mechanisms responsible for drug release have been suggested; including slightly acidic pH found in tumours, lipases from dying tumour cells and metabolization of liposomes by tumour macrophages with concurrent release of free drug [24]. Caelyx® was not approved because of increased therapeutic effect over free DXR, but due to reduced cardiac toxicities [32]. The high stability is assumed to explain the absence of improved therapeutic outcome [32]. Finding methods to destabilize liposomes within tumour tissue may therefore lead to

substantial increase in drug bioavailability with concurrent improved therapeutic outcome [24]. Several strategies have been suggested for this purpose, including rendering liposomes US-responsive [83-85].

The presence of air has for long been considered necessary to produce drug release from liposomes and different strategies have been suggested including air containing liposomes [48,49] and liposomes linked to microbubbles [50,51]. However, the large size of such structures hinders extravasation in tumours limiting their use in cancer therapies. A growing line of evidence suggests that small liposomes (~100 nm) can be made US-sensitive by manipulating membrane compositions [52,53,83-85] enabling both proper extravasation and sonosensitivity. However, US-sensitivity and high stability in blood circulation have to be counterbalanced.

The liposomal membranes of stable, long circulating liposomes like Caelyx® usually have phospatidylcholine (PC) phospholipids as a major component. Such liposomes do not respond well to US treatment as indicated in Paper II and section 5.1. However, by including the phosphatidylethanolamine (PE) phospholipid DSPE as a major fraction in the liposome membrane, liposomes can be made US-responsive (Paper I). Also, DSPE-based liposomes (Paper I) appeared to remain stable in the blood circulation as acceptable kinetic profiles were demonstrated, i.e. ~10 % of administered DXR dose was present in the blood 24 hours post injection. Such kinetic studies provide information of total DXR content in the blood and do not give direct information regarding liposome stability. However, liposome integrity is considered necessary to achieve prolonged circulation times of DXR [24] and therefore the presence of substantial DXR levels in blood 24 hours post injection indicate high stability.

Paper I also indicated that LFUS can increase the therapeutic effect of DSPE-based liposomal DXR when applied to prostate tumour xenografts 24 hours post injection. *In vitro* studies showed that LFUS induced ~20 % drug release after four minutes US treatment, presumably by destabilizing the liposomal membrane [83-85]. However, assuming that similar mechanisms could explain the enhanced therapeutic outcome is not unproblematic. Levels of dissolved gases, viscosity, purity, etc would be different in tumour tissue and it has to be expected that it would affect drug release. Further, liposome sonosensitivity may also be influenced by interaction with plasma proteins, cells, etc within tumour tissue. The observed tumour growth inhibition may therefore also result from other effects induced by US such as

heat production with increased extravasation of circulating liposomes [47], increased drug distribution in tumour tissue and increased drug uptake by cancer cells [37].

Paper II demonstrated that DOPE, a PE phospholipid traditionally used in pH-sensitive liposomes [86,87], is also suitable for rendering liposomes US-sensitive. While six minutes US treatment of DSPE-based liposomes yielded approx 25 % drug release (Paper I), identical US exposure of DOPE-based liposomes resulted in approx 90 % drug release indicating that DOPE is an even more potent modulator of sonosensitivity than DSPE. Importantly, kinetic studies demonstrated similar circulation times for liposomes comprising 25 and 32 mol % DOPE as for Caelyx® (Paper II) suggesting high stability within the blood circulation. *In vivo* liposome sonosensitivity evaluation (section 5.1) suggested that DOPE-based liposomes also expressed high US sensitivity *in vivo*. It has to be emphasised that this was a small study and robust conclusions should not be made. However, the inclusion of PE phospholipids, especially DOPE, appears to be a promising strategy for manufacturing sonosensitive liposomes that remains stable in the blood circulation as indicated by prolonged circulation times of DXR.

During preclinical therapy studies with animals bearing tumour xenografts the tumour is superficially located and easy accessed by non-focused LFUS treatment. Hence, LFUS has been used in several preclinical studies to combine with liposomal cytostatics [38,88,89]. *In vitro* studies have suggested that LFUS may be more efficient than HFUS for inducing liposomal drug release, presumably because US intensities needed to induce transient cavitation is lower at lower US frequencies [46]. Clinical implementation may, however, require non-destructive focused US of higher frequencies to enable focused deposition of acoustic energy [90,91]. Still, trends in liposome sonosensitivity have been demonstrated to be similar irrespective of US assessments have been performed with LFUS or HFUS [84,85].

Treatment of PCa is at present, among other treatment options, routinely performed by radical prostatectomy, a procedure associated with significant side effects [12]. Combining sonosensitive liposomal cytostatics with US has the potential to provide a non-invasive alternative for treating clinically localized PCa. Moreover, other localized cancers may perhaps also be treated using the technology.

6.2 Optical imaging in the development of liposomal formulations

Drug development is a long, high-risk and costly process. Out of 10.000 compounds evaluated in preclinical studies, five enter clinical trials and one receives US Food and Drug Administration (FDA) approval. The mean time from synthesis of a new compound to FDA approval is 14.2 years. For a review see [92]. Advances in imaging technologies have the potential to considerably accelerate this process [93]. During preclinical research medical imaging technologies allow biological processes to be studied *in vivo* in the same animal over a longer time interval. Such studies may reduce the number of animals needed and could potentially replace time consuming end-point analysis.

During development of new liposomal formulations assessment of tumour drug uptake is and important but time consuming process. Performing such studies with OI would enable several product candidates to be evaluated faster with less demand on animals. The biodistribution of several drug carriers have been assessed using this technology [94-101]. Such studies would in most situations require labelling with a NIR fluorochrome.

Due to the semitransparent nature of mammalian tissue light of a certain wavelength can excite exogenous applied fluorochromes within the body of small experimental animals. Upon excitation, light of a longer wavelength is emitted and can be detected on the body surface, i.e. reflectance fluorescence imaging, generating a surface map of fluorescence distribution [102].

From a practical point of view OI is cheaper, faster and easier to operate than most other imaging technologies [93,103]. Also, there is no need for radioactive agents and several animals may be imaged simultaneously generating data rapidly. However, light that passes through a medium is subjected to absorption and scattering and OI may therefore only be used for imaging depths up to one cm [102]. As tissue absorption is lowest at higher wavelengths, NIR fluorochromes are best suited for *in vivo* applications [102]. OI has been used for a variety of purposes in medical research as reviewed elsewhere [102].

In Paper III the feasibility of using OI to study liposome accumulation in tumours were evaluated. DiD-labelled PL-DXR were administered to tumour-bearing mice and tumour DiD and DXR levels determined *ex vivo* at 24 and 48 hours post injection. Analysis revealed

higher levels of DXR than DiD in the blood at both 24 and 48 hours indicating dissociation of DiD from liposomes in the blood circulation. *In vivo* fluorescence acquisitions will under such circumstances not only image labelled liposomes but also dissociated dye. Moreover, only a weak association was observed between *in vivo* DiD tumour fluorescence intensity and actual tumour DiD levels (R^2=0.59). The absence of a strong correlation was presumably due to absorption and scattering of *in vivo* DiD tumour fluorescence [102,104]. However, during image analysis the ROI is drawn manually along the edges of the tumour and poorly visible tumour margins may impede drawing of ROI. Also, fluorescence emitted from outside ROI may also preclude measurements. Consequently, several factors may have in combination reduced the sensitivity of the assay.

Even if quantifying liposomal tumour uptake in absolute numbers may not be possible with OI, relative differences in tumour uptake between different liposomal formulations could perhaps be successfully evaluated on condition that there is no dissociation of the labelling fluorochrome within the blood circulation and that tumours are reasonably homogenous in size and shape.

During development of drug containing sonosensitive liposomes sufficient drug release at target site should be evaluated. Extent of *in vitro* drug release from liposomes can be determined as described in Paper I and II. The extent of drug release *in vivo* is somewhat more complicated to evaluate. However, OI might be a promising method for this purpose as indicated in Section 5.1.

6.3 Liposomal doxorubicin in combined chemoradioterapy

During tumour growth impaired blood supply fail to deliver sufficient amounts of oxygen to growing tumours resulting in various degrees of hypoxia [55,56]. Hypoxia reduces the effect of RT and several strategies have been suggested to improve RT under hypoxic conditions [60,61].

Combining cytostatics with RT is used in the treatment of cancers to achieve increased efficacy [62,105]. DXR is a potent radiosensitizer and enhance the effect of RT presumably by inhibiting repair mechanisms following radiation induced DNA damage [64,65,106]. It has also been suggested that DXR reoxygenate tumours by reducing oxygen consumption in

tumour cells [107,108] rendering the tumour more sensitive to RT. Clinical studies have reported promising results by combining RT with conventional DXR in the treatment of various sarcomas [109-113]. However, as tumour tissue favours accumulation of liposomes, using PL-DXR in CRT may enhance efficacy primarily in tumour tissue [66].

Preclinical CRT studies, involving both PL-DXR [66,68] and non-pegylated liposomal DXR [69], have described enhanced therapeutic effects when combined with RT. Combining PL-DXR with RT in clinical studies have also been performed. However, due to low number of patients and the simultaneous inclusion of other therapeutic agents in addition to PL-DXR and RT, assessing the beneficial effect of PL-DXR in some of these studies is somewhat difficult. Nevertheless, promising results are described for several cancers including breast cancer [114,115], sarcomas [67], non-small cell lung cancer [70,116,117], head and neck cancer [70], glioblastoma and metastatic brain tumours [118]. Also, less promising results are reported for non-small cell lung cancer [119] and glioblastoma [120]. However, according to my knowledge there has not been performed any major randomized trials with CRT involving PL-DXR.

Even though conventional DXR is reported to enhance the effect of RT, it is also reported to reduce tumour blood flow [121,122], presumably by inducing endothelial damage with concurrent vascular dysfunction [123-125]. In contrast, PL-DXR is reported to normalize tumour blood flow [126] indicating that PL-DXR may be beneficial in CRT not only by increasing the effect of RT primarily in tumour tissue but also by reducing DXR mediated adverse effects on tumour vascular functions. As suggested in Paper IV, PL-DXR produced therapeutic effect without significantly altering tumour vascular functions as judged by DCE MRI and immunohistochemistry. For co-administration with RT this is beneficial because well vascularised tumours may have less degree of hypoxia. The presence of oxygen in tumours is vital due to 1) the production of radicals and thus DNA damage and 2) to prevent DNA repair by fixating the damage [127]. DXR may therefore resemble oxygen in tumours exposed to RT. It has to be emphasised that this study was performed using a drug dose of 3.5 mg DXR/kg and the result may not be valid for other drug doses. Other drug doses may, perhaps, produce vascular alterations limiting tumour blood flow.

Hypoxia is a common feature of most tumours [127] and the ability to achieve effective RT under hypoxic conditions is therefore of great importance. Paper IV demonstrated that the

effect of RT is greatly reduced by hypoxia. Here, hypoxia was induced by clamping the tumour-bearing leg creating ischemia with concurrent hypoxia. It has to be anticipated that temporary episodes of acute hypoxia induced this way would differ from hypoxia in clinical tumours. However, the concomitant administration of PL-DXR improved therapeutic outcome indicating that PL-DXR may increase the effect of RT under hypoxic conditions.

Overcoming hypoxia by administering radiosensitizing drugs may be of limited value as supply to hypoxic regions are commonly reduced by inadequate vascularisation. However, PL-DXR seems to have a positive effect on vascular functions as suggested in paper IV. Here, vascular alterations induced by hypoxic RT were apparently reduced by co-administration of PL-DXR as judged by DCE MRI.

Data analysis of DCE MRI was performed by identifying three kinetic parameters A, K_{ep} and K_{el} (Paper IV). However, the K_{ep} parameter, which identifies the transfer rate between plasma and EES, had to be excluded from the study as non-physiological values were generated both pre and post treatment. Rapid contrast agent in-wash originating from high permeability and/or high perfusion could provide an explanation. Moreover, methodological limitations may also be suggested. I.e. registering contrast transfer between plasma and EES is influenced by the speed of contrast administration [75]. Also, limitations in time resolution could further explain why the kinetic model did not generate meaningful K_{ep} values. Due to unsuccessful contrast administration or tumour sizes being too small to enable reliable DCE MRI analysis it was not possible to generate A and K_{el} values for all animals that entered the study.

DXR exert cytotoxic effects by interfering with several cellular processes [128] and numerous mechanisms may explain the radiosensitizing properties of DXR. However, as all tumours have some degrees of hypoxia [129], the ability of PL-DXR to increase the effect of RT under hypoxic conditions could provide some explanation to why PL-DXR increase the effect of RT. For drugs that affect tumour vascular functions liposomes may be an interesting drug delivery technology for use in CRT.

To my knowledge there have been no clinical studies on CRT involving PL-DXR on PCa. Even though results obtained from preclinical studies frequently fail in predicting clinical results [82], the ability of PL-DXR to increase the effect of RT under hypoxic conditions in

xenograft models are nontrivial as it is well documented that hypoxia reduces the effect of RT in PCa [57-59].

6. Conclusions

The work presented in this thesis suggests that PL-DXR can produce enhanced effects when combined with other treatment modalities, i.e. US and RT, as judged by assessment in preclinical models. Further, OI appears not to be promising for performing biodistribution studies of fluorescence labelled liposomes. The following conclusions can be made:

• Including DSPE as a major fraction in the liposomal membrane can render liposomes US-sensitive with acceptable circulation time.

• LFUS can enhance the therapeutic effect of DSPE-based liposomal DXR in mice bearing prostate cancer xenografts. However, the benefit of LFUS treatment appears to be modest but statistically significant.

• DOPE appears to be a potent modulator for sonosensitivity. However, high DOPE content reduces liposome stability in the blood stream.

• Dissociation of DiD from liposomes in the blood stream limits the suitability of DiD as a marker for liposomes *in vivo*.

• Scattering and absorption of light limits the usefulness of OI for assessing the biodistribution profile of fluorescence labelled liposomes.

• PL-DXR induces antitumour effect apparently without influencing tumour vascular functions at a dose of 3.5 mg DXR/kg. Further, PL-DXR appears to reduce some of the vascular alterations induced in hypoxic tumours by RT.

• PL-DXR increases the therapeutic effect of RT in radioresistant tumour xenografts.

7. Perspectives

This thesis has demonstrated that antitumour effect of sonosensitive liposomal DXR in animal models can be enhanced by concurrent LFUS treatment. However, further manipulation of liposome membrane composition may generate sonosensitive liposomes with properties superior to those described in this thesis. Also, focused US of higher frequencies may be used to restrict acoustic cavitation to tumour tissue. Therapeutic assessment of DOPE-based liposomal DXR and US of higher frequencies (500 kHz - 1.13 MHz) will be tested in mice bearing prostate and breast cancer xenografts in near future.

Studying liposomal biodistribution by OI demands strong bonding between liposome and labelling fluorochrome. As DiD appears to dissociate *in vivo*, finding stable labelling techniques may improve quality of assay. However, it has to be anticipated that liposomes at some time post injection will disintegrate. In such case the labelling fluorochrome will no longer label intact liposomes. Consequently, it has to be questioned whether OI is a suitable technique for studying the biodistribution profile of labelled liposomes.

Several reports have demonstrated that PL-DXR increases the effect of RT, also under hypoxic condition as suggested in this thesis. However, using other drug doses or different time intervals between drug administration and start of RT may improve therapeutic outcome. As the biodistribution profiles of drugs are changed by liposomal encapsulation, encapsulating other radiosensitizing drugs may perhaps be an interesting drug delivery strategy.

8. References

(1) Ferlay J, Shin HR, Bray F, Forman D, Mathers C, and Parkin DM (2010). Estimates of worldwide burden of cancer in 2008: GLOBOCAN 2008. *Int J Cancer.* **127**, 2893-2917.

(2) Cancer in Norway (2008). Cancer registry of Norway.

(3) Weinberg RA (2007). The biology of cancer. Garland Science, NY, USA.

(4) Jang SH, Wientjes MG, Lu D, and Au JL (2003). Drug delivery and transport to solid tumors. *Pharm Res.* **20**, 1337-1350.

(5) Tannock IF (2001). Tumor physiology and drug resistance. *Cancer Metastasis Rev.* **20**, 123-132.

(6) Becker WM (2006). The world of the cell, 6th edition. Pearson Education, San Fransisco, CA.

(7) American Joint Committee on Cancer.: AJCC Cancer Staging Manual 6th ed. (2002). Springer, NY.

(8) Gleason DF, and Mellinger GT (1974). Prediction of prognosis for prostatic adenocarcinoma by combined histological grading and clinical staging. *J Urol.* **111**, 58-64.

(9) Heidenreich A, Aus G, Bolla M, Joniau S, Matveev VB, Schmid HP, and Zattoni F (2008). EAU guidelines on prostate cancer. *Eur Urol.* **53**, 68-80.

(10) Heinzer H, and Steuber T (2009). Prostate cancer in the elderly. *Urol Oncol.* **27**, 668-672.

(11) Horwich A, Parker C, Bangma C, and Kataja V (2010). Prostate cancer: ESMO Clinical Practice Guidelines for diagnosis, treatment and follow-up. *Ann Oncol.* **21 Suppl 5**, v129-v133.

(12) www.oncolex.no (2011)

(13) Maestroni U, Ziveri M, Azzolini N, Dinale F, Ziglioli F, Campaniello G, Frattini A, and Ferretti S (2008). High Intensity Focused Ultrasound (HIFU): a useful alternative choice in prostate cancer treatment. Preliminary results. *Acta Biomed.* **79**, 211-216.

(14) Thuroff S, Chaussy C, Vallancien G, Wieland W, Kiel HJ, Le DA, Desgrandchamps F, De La Rosette JJ, and Gelet A (2003). High-intensity focused ultrasound and localized prostate cancer: efficacy results from the European multicentric study. *J Endourol.* **17**, 673-677.

(15) Park SY, Kim YJ, Gao AC, Mohler JL, Onate SA, Hidalgo AA, Ip C, Park EM, Yoon SY, and Park YM (2006). Hypoxia increases androgen receptor activity in prostate cancer cells. *Cancer Res.* **66**, 5121-5129.

(16) Damber JE, and Aus G (2008). Prostate cancer. *Lancet.* **371**, 1710-1721.

(17) New RRC (1990). Liposomes: A Practical Approach. Oxford University Press, NY, USA.

(18) Kulkarni SB, Betageri GV, and Singh M (1995). Factors affecting microencapsulation of drugs in liposomes. *J Microencapsul.* **12**, 229-246.

(19) Bangham AD, Standish MM, and Watkins JC (1965). Diffusion of univalent ions across the lamellae of swollen phospholipids. *J Mol Biol.* **13**, 238-252.

(20) Torchilin VP (2005). Recent advances with liposomes as pharmaceutical carriers. *Nat Rev Drug Discov.* **4**, 145-160.

(21) Maeda H, Wu J, Sawa T, Matsumura Y, and Hori K (2000). Tumor vascular permeability and the EPR effect in macromolecular therapeutics: a review. *J Control Release.* **65**, 271-284.

(22) Gabizon A, Shmeeda H, and Barenholz Y (2003). Pharmacokinetics of pegylated liposomal Doxorubicin: review of animal and human studies. *Clin Pharmacokinet.* **42**, 419-436.

(23) Weiss RB (1992). The anthracyclines: will we ever find a better doxorubicin? *Semin Oncol.* **19**, 670-686.

(24) Drummond DC, Meyer O, Hong K, Kirpotin DB, and Papahadjopoulos D (1999). Optimizing liposomes for delivery of chemotherapeutic agents to solid tumors. *Pharmacol Rev.* **51**, 691-743.

(25) Batist G (2007). Cardiac safety of liposomal anthracyclines. *Cardiovasc Toxicol.* **7**, 72-74.

(26) Ewer MS, Martin FJ, Henderson C, Shapiro CL, Benjamin RS, and Gabizon AA (2004). Cardiac safety of liposomal anthracyclines. *Semin Oncol.* **31**, 161-181.

(27) Heidenreich A, Sommer F, Ohlmann CH, Schrader AJ, Olbert P, Goecke J, and Engelmann UH (2004). Prospective randomized Phase II trial of pegylated doxorubicin in the management of symptomatic hormone-refractory prostate carcinoma. *Cancer.* **101**, 948-956.

(28) Fossa SD, Vaage S, Letocha H, Iversen J, Risberg T, Johannessen DC, Paus E, and Smedsrud T (2002). Liposomal doxorubicin (Caelyx) in symptomatic androgen-independent prostate cancer (AIPC)--delayed response and flare phenomenon should be considered. *Scand J Urol Nephrol.* **36**, 34-39.

(29) Hubert A, Lyass O, Pode D, and Gabizon A (2000). Doxil (Caelyx): an exploratory study with pharmacokinetics in patients with hormone-refractory prostate cancer. *Anticancer Drugs.* **11**, 123-127.

(30) McMenemin R, Macdonald G, Moffat L, and Bissett D (2002). A phase II study of caelyx (liposomal doxorubicin) in metastatic carcinoma of the prostate: tolerability and efficacy modification by liposomal encapsulation. *Invest New Drugs.* **20**, 331-337.

(31) Horowitz AT, Barenholz Y, and Gabizon AA (1992). In vitro cytotoxicity of liposome-encapsulated doxorubicin: dependence on liposome composition and drug release. *Biochim Biophys Acta.* **1109**, 203-209.

(32) Lindner LH, and Hossann M (2010). Factors affecting drug release from liposomes. *Curr Opin Drug Discov Devel.* **13**, 111-123.

(33) Needham D, and Dewhirst MW (2001). The development and testing of a new temperature-sensitive drug delivery system for the treatment of solid tumors. *Adv Drug Deliv Rev.* **53**, 285-305.

(34) Davidsen J, Vermehren C, Frokjaer S, Mouritsen OG, and Jorgensen K (2001). Drug delivery by phospholipase A(2) degradable liposomes. *Int J Pharm.* **214**, 67-69.

(35) Sudimack JJ, Guo W, Tjarks W, and Lee RJ (2002). A novel pH-sensitive liposome formulation containing oleyl alcohol. *Biochim Biophys Acta.* **1564**, 31-37.

(36) Schroeder A, Avnir Y, Weisman S, Najajreh Y, Gabizon A, Talmon Y, Kost J, and Barenholz Y (2007). Controlling liposomal drug release with low frequency ultrasound: mechanism and feasibility. *Langmuir.* **23**, 4019-4025.

(37) Pitt WG, Husseini GA, and Staples BJ (2004). Ultrasonic drug delivery--a general review. *Expert Opin Drug Deliv.* **1**, 37-56.

(38) Schroeder A, Honen R, Turjeman K, Gabizon A, Kost J, and Barenholz Y (2009). Ultrasound triggered release of cisplatin from liposomes in murine tumors. *J Control Release.* **137**, 63-68.

(39) Liang HD, and Blomley MJ (2003). The role of ultrasound in molecular imaging. *Br J Radiol.* **76 Spec No 2**, S140-S150.

(40) Mason TJ (2011). Therapeutic ultrasound an overview. *Ultrason Sonochem.* **18**, 847-852.

(41) Finley DS, Pouliot F, Shuch B, Chin A, Pantuck A, Dekernion JB, and Belldegrun AS (2011). Ultrasound-based combination therapy: potential in urologic cancer. *Expert Rev Anticancer Ther.* **11**, 107-113.

(42) Stewart EA, Gedroyc WM, Tempany CM, Quade BJ, Inbar Y, Ehrenstein T, Shushan A, Hindley JT, Goldin RD, David M, Sklair M, and Rabinovici J (2003). Focused ultrasound treatment of uterine fibroid tumors: safety and feasibility of a noninvasive thermoablative technique. *Am J Obstet Gynecol.* **189**, 48-54.

(43) Sundaram J, Mellein BR, and Mitragotri S (2003). An experimental and theoretical analysis of ultrasound-induced permeabilization of cell membranes. *Biophys J.* **84**, 3087-3101.

(44) Postema M, and Gilja OH (2007). Ultrasound-directed drug delivery. *Curr Pharm Biotechnol.* **8**, 355-361.

(45) Frenkel V (2008). Ultrasound mediated delivery of drugs and genes to solid tumors. *Adv Drug Deliv Rev.* **60**, 1193-1208.

(46) Schroeder A, Kost J, and Barenholz Y (2009). Ultrasound, liposomes, and drug delivery: principles for using ultrasound to control the release of drugs from liposomes. *Chem Phys Lipids.* **162**, 1-16.

(47) Kong G, Braun RD, and Dewhirst MW (2001). Characterization of the effect of hyperthermia on nanoparticle extravasation from tumor vasculature. *Cancer Res.* **61**, 3027-3032.

(48) Huang SL, and MacDonald RC (2004). Acoustically active liposomes for drug encapsulation and ultrasound-triggered release. *Biochim Biophys Acta.* **1665**, 134-141.

(49) Huang SL, McPherson DD, and Macdonald RC (2008). A method to co-encapsulate gas and drugs in liposomes for ultrasound-controlled drug delivery. *Ultrasound Med Biol.* **34**, 1272-1280.

(50) Lentacker I, Geers B, Demeester J, De Smedt SC, and Sanders NN (2010). Design and evaluation of doxorubicin-containing microbubbles for ultrasound-triggered doxorubicin delivery: cytotoxicity and mechanisms involved. *Mol Ther.* **18**, 101-108.

(51) Kheirolomoom A, Dayton PA, Lum AF, Little E, Paoli EE, Zheng H, and Ferrara KW (2007). Acoustically-active microbubbles conjugated to liposomes: characterization of a proposed drug delivery vehicle. *J Control Release.* **118**, 275-284.

(52) Lin HY, and Thomas JL (2004). Factors affecting responsivity of unilamellar liposomes to 20 kHz ultrasound. *Langmuir.* **20**, 6100-6106.

(53) Lin HY, and Thomas JL (2003). PEG-Lipids and Oligo(ethylene glycol) Surfactants Enhance the Ultrasonic Permeabilizability of Liposomes. *Langmuir.* **19**, 1098-1105.

(54) Pong M, Umchid S, Guarino AJ, Lewin PA, Litniewski J, Nowicki A, and Wrenn SP (2006). In vitro ultrasound-mediated leakage from phospholipid vesicles. *Ultrasonics.* **45**, 133-145.

(55) Hockel M, and Vaupel P (2001). Tumor hypoxia: definitions and current clinical, biologic, and molecular aspects. *J Natl Cancer Inst.* **93**, 266-276.

(56) Vaupel P, Kelleher DK, and Hockel M (2001). Oxygen status of malignant tumors: pathogenesis of hypoxia and significance for tumor therapy. *Semin Oncol.* **28**, 29-35.

(57) Marignol L, Coffey M, Lawler M, and Hollywood D (2008). Hypoxia in prostate cancer: a powerful shield against tumour destruction? *Cancer Treat Rev.* **34**, 313-327.

(58) Rudolfsson SH, and Bergh A (2009). Hypoxia drives prostate tumour progression and impairs the effectiveness of therapy, but can also promote cell death and serve as a therapeutic target. *Expert Opin Ther Targets.* **13**, 219-225.

(59) Stewart GD, Ross JA, McLaren DB, Parker CC, Habib FK, and Riddick AC (2010). The relevance of a hypoxic tumour microenvironment in prostate cancer. *BJU Int.* **105**, 8-13.

(60) Overgaard J (2007). Hypoxic radiosensitization: adored and ignored. *J Clin Oncol.* **25**, 4066-4074.

(61) Wouters BG, Weppler SA, Koritzinsky M, Landuyt W, Nuyts S, Theys J, Chiu RK, and Lambin P (2002). Hypoxia as a target for combined modality treatments. *Eur J Cancer.* **38**, 240-257.

(62) Seiwert TY, Salama JK, and Vokes EE (2007). The concurrent chemoradiation paradigm--general principles. *Nat Clin Pract Oncol.* **4**, 86-100.

(63) Bellamy AS, and Hill BT (1984). Interactions between clinically effective antitumor drugs and radiation in experimental systems. *Biochim Biophys Acta.* **738**, 125-166.

(64) Bonner JA, and Lawrence TS (1990). Doxorubicin decreases the repair of radiation-induced DNA damage. *Int J Radiat Biol.* **57**, 55-64.

(65) Byfield JE, Lynch M, Kulhanian F, and Chan PY (1977). Cellular effects of combined adriamycin and x-irradiation in human tumor cells. *Int J Cancer.* **19**, 194-204.

(66) Harrington KJ, Rowlinson-Busza G, Syrigos KN, Vile RG, Uster PS, Peters AM, and Stewart JS (2000). Pegylated liposome-encapsulated doxorubicin and cisplatin enhance the effect of radiotherapy in a tumor xenograft model. *Clin Cancer Res.* **6**, 4939-4949.

(67) Koukourakis MI, Koukouraki S, Giatromanolaki A, Kakolyris S, Georgoulias V, Velidaki A, Archimandritis S, and Karkavitsas NN (2000). High intratumoral accumulation of stealth liposomal doxorubicin in sarcomas--rationale for combination with radiotherapy. *Acta Oncol.* **39**, 207-211.

(68) Davies CL, Lundstrom LM, Frengen J, Eikenes L, Bruland S OS, Kaalhus O, Hjelstuen MH, and Brekken C (2004). Radiation improves the distribution and uptake of liposomal doxorubicin (caelyx) in human osteosarcoma xenografts. *Cancer Res.* **64**, 547-553.

(69) Labussiere M, Aarnink A, Pinel S, Taillandier L, Escanye JM, Barberi-Heyob M, Bernier-Chastagner V, Plenat F, and Chastagner P (2008). Interest of liposomal doxorubicin as a radiosensitizer in malignant glioma xenografts. *Anticancer Drugs.* **19**, 991-998.

(70) Koukourakis MI, Koukouraki S, Giatromanolaki A, Archimandritis SC, Skarlatos J, Beroukas K, Bizakis JG, Retalis G, Karkavitsas N, and Helidonis ES (1999). Liposomal doxorubicin and conventionally fractionated radiotherapy in the treatment of locally advanced non-small-cell lung cancer and head and neck cancer. *J Clin Oncol.* **17**, 3512-3521.

(71) Pretlow TG, Wolman SR, Micale MA, Pelley RJ, Kursh ED, Resnick MI, Bodner DR, Jacobberger JW, Delmoro CM, Giaconia JM, and . (1993). Xenografts of primary human prostatic carcinoma. *J Natl Cancer Inst.* **85**, 394-398.

(72) Sramkoski RM, Pretlow TG, Giaconia JM, Pretlow TP, Schwartz S, Sy MS, Marengo SR, Rhim JS, Zhang D, and Jacobberger JW (1999). A new human prostate carcinoma cell line, 22Rv1. *In Vitro Cell Dev Biol Anim.* **35**, 403-409.

(73) Roe K, Seierstad T, Kristian A, Mikalsen LT, Maelandsmo GM, van der Kogel AJ, Ree AH, and Olsen DR (2010). Longitudinal magnetic resonance imaging-based

assessment of vascular changes and radiation response in androgen-sensitive prostate carcinoma xenografts under androgen-exposed and androgen-deprived conditions. *Neoplasia.* **12**, 818-825.

(74) Seierstad T, Roe K, and Hovik B (2007). Construction of a modified capacitive overlap MR coil for imaging of small animals and objects in a clinical whole-body scanner. *Phys Med Biol.* **52**, N513-N522.

(75) Brix G, Semmler W, Port R, Schad LR, Layer G, and Lorenz WJ (1991). Pharmacokinetic parameters in CNS Gd-DTPA enhanced MR imaging. *J Comput Assist Tomogr.* **15**, 621-628.

(76) Markwardt CB (2008). Non-Linear Least Squares Fitting in IDL with MPFIT. *proc Astronomical Data Analysis Software and Systems XVIII, Quebec, Canada, ASP Conference Series.* **411**, 251-254.

(77) Sovik S, Skogmo HK, Andersen EK, Bruland OS, Olsen DR, and Malinen E (2009). DCEMRI of spontaneous canine tumors during fractionated radiotherapy: a pharmacokinetic analysis. *Radiother Oncol.* **93**, 618-624.

(78) Chen RF, and Knutson JR (1988). Mechanism of fluorescence concentration quenching of carboxyfluorescein in liposomes: energy transfer to nonfluorescent dimers. *Anal Biochem.* **172**, 61-77.

(79) Krishna R, Ghiu G, and Mayer LD (2001). Visualization of bioavailable liposomal doxorubicin using a non-perturbing confocal imaging technique. *Histol Histopathol.* **16**, 693-699.

(80) Mermut O, Noiseux I, Bouchard JP, Cormier JF, Desroches P, Fortin M, Gallant P, Leclair S, Vernon ML, Diamond KR, and Patterson MS (2008). Effect of liposomal confinement on photothermal and photo-oximetric fluorescence lifetimes of photosensitizers with varying hydrophilicity. *J Biomed Opt.* **13**, 041314.

(81) Charrois GJ, and Allen TM (2004). Drug release rate influences the pharmacokinetics, biodistribution, therapeutic activity, and toxicity of pegylated liposomal doxorubicin formulations in murine breast cancer. *Biochim Biophys Acta.* **1663**, 167-177.

(82) Suthar MP, and Javia A (2009). Xenograft cancer mice models in cancer drug discovery. *Pharma Times.* **41**, 15-19.

(83) Evjen TJ, Nilssen EA, Rognvaldsson S, Brandl M, and Fossheim SL (2010). Distearoylphosphatidylethanolamine-based liposomes for ultrasound-mediated drug delivery. *Eur J Pharm Biopharm.* **75**, 327-333.

(84) Evjen TJ, Nilssen EA, Fowler RA, Rognvaldsson S, Brandl M, and Fossheim SL (2011). Lipid membrane composition influences drug release from dioleoylphosphatidylethanolamine-based liposomes on exposure to ultrasound. *Int J Pharm.* **406**, 114-116.

(85) Evjen TJ, Nilssen EA, Barnert S, Schubert R, Brandl M, and Fossheim SL (2011). Ultrasound-mediated destabilization and drug release from liposomes comprising dioleoylphosphatidylethanolamine. *Eur J Pharm Sci.* **42**, 380-386.

(86) De Oliveira MC, Fattal E, Couvreur P, Lesieur P, Bourgaux C, Ollivon M, and Dubernet C (1998). pH-sensitive liposomes as a carrier for oligonucleotides: a physico-chemical study of the interaction between DOPE and a 15-mer oligonucleotide in quasi-anhydrous samples. *Biochim Biophys Acta.* **1372**, 301-310.

(87) Slepushkin VA, Simoes S, Dazin P, Newman MS, Guo LS, Pedroso de Lima MC, and Duzgunes N (1997). Sterically stabilized pH-sensitive liposomes. Intracellular delivery of aqueous contents and prolonged circulation in vivo. *J Biol Chem.* **272**, 2382-2388.

(88) Pitt WG, Husseini GA, Roeder BL, Dickinson DJ, Warden DR, Hartley JM, and Jones PW (2011). Preliminary results of combining low frequency low intensity ultrasound and liposomal drug delivery to treat tumors in rats. *J Nanosci Nanotechnol.* **11**, 1866-1870.

(89) Myhr G, and Moan J (2006). Synergistic and tumour selective effects of chemotherapy and ultrasound treatment. *Cancer Lett.* **232**, 206-213.

(90) Wang S, Zderic V, and Frenkel V (2010). Extracorporeal, low-energy focused ultrasound for noninvasive and nondestructive targeted hyperthermia. *Future Oncol.* **6**, 1497-1511.

(91) Yuh EL, Shulman SG, Mehta SA, Xie J, Chen L, Frenkel V, Bednarski MD, and Li KC (2005). Delivery of systemic chemotherapeutic agent to tumors by using focused ultrasound: study in a murine model. *Radiology.* **234**, 431-437.

(92) Willmann JK, van BN, Dinkelborg LM, and Gambhir SS (2008). Molecular imaging in drug development. *Nat Rev Drug Discov.* **7**, 591-607.

(93) Rudin M, and Weissleder R (2003). Molecular imaging in drug discovery and development. *Nat Rev Drug Discov.* **2**, 123-131.

(94) Almutairi A, Akers WJ, Berezin MY, Achilefu S, and Frechet JM (2008). Monitoring the biodegradation of dendritic near-infrared nanoprobes by in vivo fluorescence imaging. *Mol Pharm.* **5**, 1103-1110.

(95) Corbin IR, Chen J, Cao W, Li H, Lund-Katz S, and Zheng G (2007). Enhanced Cancer-Targeted Delivery Using Engineered High-Density Lipoprotein-Based Nanocarriers. *Journal of Biomedical Nanotechnology.* **3**, 367-376.

(96) Deissler V, Ruger R, Frank W, Fahr A, Kaiser WA, and Hilger I (2008). Fluorescent liposomes as contrast agents for in vivo optical imaging of edemas in mice. *Small.* **4**, 1240-1246.

(97) Ghoroghchian PP, Frail PR, Susumu K, Blessington D, Brannan AK, Bates FS, Chance B, Hammer DA, and Therien MJ (2005). Near-infrared-emissive polymersomes: self-assembled soft matter for in vivo optical imaging. *Proc Natl Acad Sci U S A.* **102**, 2922-2927.

(98) Li H, Zhang Z, Blessington D, Nelson DS, Zhou R, Lund-Katz S, Chance B, Glickson JD, and Zheng G (2004). Carbocyanine labeled LDL for optical imaging of tumors. *Acad Radiol.* **11**, 669-677.

(99) Liang M, Liu X, Cheng D, Liu G, Dou S, Wang Y, Rusckowski M, and Hnatowich DJ (2010). Multimodality nuclear and fluorescence tumor imaging in mice using a streptavidin nanoparticle. *Bioconjug Chem.* **21**, 1385-1388.

(100) Quadir MA, Radowski MR, Kratz F, Licha K, Hauff P, and Haag R (2008). Dendritic multishell architectures for drug and dye transport. *J Control Release.* **132**, 289-294.

(101) Goutayer M, Dufort S, Josserand V, Royere A, Heinrich E, Vinet F, Bibette J, Coll JL, and Texier I (2010). Tumor targeting of functionalized lipid nanoparticles: assessment by in vivo fluorescence imaging. *Eur J Pharm Biopharm.* **75**, 137-147.

(102) Licha K, and Olbrich C (2005). Optical imaging in drug discovery and diagnostic applications. *Adv Drug Deliv Rev.* **57**, 1087-1108.

(103) Rice BW, Cable MD, and Nelson MB (2001). In vivo imaging of light-emitting probes. *J Biomed Opt.* **6**, 432-440.

(104) Ntziachristos V, Bremer C, and Weissleder R (2003). Fluorescence imaging with near-infrared light: new technological advances that enable in vivo molecular imaging. *Eur Radiol.* **13**, 195-208.

(105) Tannock IF (1996). Treatment of cancer with radiation and drugs. *J Clin Oncol.* **14**, 3156-3174.

(106) Watring WG, Byfield JE, Lagasse LD, Lee YD, Juillard G, Jacobs M, and Smith ML (1974). Combination Adriamycin and radiation therapy in gynecologic cancers. *Gynecol Oncol.* **2**, 518-526.

(107) Gosalvez M, Blanco M, Hunter J, Miko M, and Chance B (1974). Effects of anticancer agents on the respiration of isolated mitochondria and tumor cells. *Eur J Cancer.* **10**, 567-574.

(108) Durand RE (1976). Adriamycin: a possible indirect radiosensitizer of hypoxic tumor cells. *Radiology.* **119**, 217-222.

(109) Toma S, Canavese G, Grimaldi A, Ravera G, Ugolini D, Percivale P, and Badellino F (2003). Concomitant chemo-radiotherapy in the treatment of locally advanced and/or metastatic soft tissue sarcomas: experience of the National Cancer Institute of Genoa. *Oncol Rep.* **10**, 641-647.

(110) Pisters PW, Ballo MT, Fenstermacher MJ, Feig BW, Hunt KK, Raymond KA, Burgess MA, Zagars GK, Pollock RE, Benjamin RS, and Patel SR (2003). Phase I trial of preoperative concurrent doxorubicin and radiation therapy, surgical resection, and intraoperative electron-beam radiation therapy for patients with localized retroperitoneal sarcoma. *J Clin Oncol.* **21**, 3092-3097.

(111) Sordillo PP, Magill GB, Schauer PK, Vikram B, Kim JH, and Hilaris BS (1982). Preliminary trial of combination therapy with adriamycin and radiation in sarcomas and other malignant tumors. *J Surg Oncol.* **21**, 23-26.

(112) Rosenthal CJ, and Rotman M (1988). Pilot study of interaction of radiation therapy with doxorubicin by continuous infusion. *NCI Monogr.*: 285-290.

(113) Toma S, Palumbo R, Sogno G, Canavese G, Barra S, Marziano C, Serrano J, Albanese E, and Rosso R (1991). Concomitant radiation-doxorubicin administration in locally advanced and/or metastatic soft tissue sarcomas: preliminary results. *Anticancer Res.* **11**, 2085-2089.

(114) Kouloulias VE, Dardoufas CE, Kouvaris JR, Gennatas CS, Polyzos AK, Gogas HJ, Sandilos PH, Uzunoglu NK, Malas EG, and Vlahos LJ (2002). Liposomal doxorubicin in conjunction with reirradiation and local hyperthermia treatment in recurrent breast cancer: a phase I/II trial. *Clin Cancer Res.* **8**, 374-382.

(115) Koukourakis MI, Manavis J, Simopoulos C, Liberis V, Giatromanolaki A, and Sivridis E (2005). Hypofractionated accelerated radiotherapy with cytoprotection combined with trastuzumab, liposomal doxorubicine, and docetaxel in c-erbB-2-positive breast cancer. *Am J Clin Oncol.* **28**, 495-500.

(116) Koukourakis MI, Patlakas G, Froudarakis ME, Kyrgias G, Skarlatos J, Abatzoglou I, Bougioukas G, and Bouros D (2007). Hypofractionated accelerated radiochemotherapy with cytoprotection (Chemo-HypoARC) for inoperable non-small cell lung carcinoma. *Anticancer Res.* **27**, 3625-3631.

(117) Koukourakis MI, Romanidis K, Froudarakis M, Kyrgias G, Koukourakis GV, Retalis G, and Bahlitzanakis N (2002). Concurrent administration of Docetaxel and Stealth liposomal doxorubicin with radiotherapy in non-small cell lung cancer : excellent tolerance using subcutaneous amifostine for cytoprotection. *Br J Cancer.* **87**, 385-392.

(118) Koukourakis MI, Koukouraki S, Fezoulidis I, Kelekis N, Kyrias G, Archimandritis S, and Karkavitsas N (2000). High intratumoural accumulation of stealth liposomal doxorubicin (Caelyx) in glioblastomas and in metastatic brain tumours. *Br J Cancer.* **83**, 1281-1286.

(119) Tsoutsou PG, Froudarakis ME, Bouros D, and Koukourakis MI (2008). Hypofractionated/accelerated radiotherapy with cytoprotection (HypoARC) combined with vinorelbine and liposomal doxorubicin for locally advanced non-small cell lung cancer (NSCLC). *Anticancer Res.* **28**, 1349-1354.

(120) Beier CP, Schmid C, Gorlia T, Kleinletzenberger C, Beier D, Grauer O, Steinbrecher A, Hirschmann B, Brawanski A, Dietmaier C, Jauch-Worley T, Kolbl O, Pietsch T, Proescholdt M, Rummele P, Muigg A, Stockhammer G, Hegi M, Bogdahn U, and Hau P (2009). RNOP-09: pegylated liposomal doxorubicine and prolonged temozolomide in addition to radiotherapy in newly diagnosed glioblastoma--a phase II study. *BMC Cancer.* **9**, 308.

(121) Durand RE, and LePard NE (1994). Modulation of tumor hypoxia by conventional chemotherapeutic agents. *Int J Radiat Oncol Biol Phys.* **29**, 481-486.

(122) Durand RE, and LePard NE (1997). Tumour blood flow influences combined radiation and doxorubicin treatments. *Radiother Oncol.* **42**, 171-179.

(123) Murata T, Yamawaki H, Hori M, Sato K, Ozaki H, and Karaki H (2001). Chronic vascular toxicity of doxorubicin in an organ-cultured artery. *Br J Pharmacol.* **132**, 1365-1373.

(124) Olukman M, Can C, Erol A, Oktem G, Oral O, and Cinar MG (2009). Reversal of doxorubicin-induced vascular dysfunction by resveratrol in rat thoracic aorta: Is there a possible role of nitric oxide synthase inhibition? *Anadolu Kardiyol Derg.* **9**, 260-266.

(125) Wolf MB, and Baynes JW (2006). The anti-cancer drug, doxorubicin, causes oxidant stress-induced endothelial dysfunction. *Biochim Biophys Acta.* **1760**, 267-271.

(126) Verreault M, Strutt D, Masin D, Anantha M, Yung A, Kozlowski P, Waterhouse D, Bally MB, and Yapp DT (2011). Vascular normalization in orthotopic glioblastoma following intravenous treatment with lipid-based nanoparticulate formulations of irinotecan (Irinophore C), doxorubicin (Caelyx(R)) or vincristine. *BMC Cancer.* **11**, 124.

(127) Bussink J, Kaanders JH, van der Graaf WT, and Oyen WJ (2011). PET-CT for radiotherapy treatment planning and response monitoring in solid tumors. *Nat Rev Clin Oncol.* **8**, 233-242.

(128) Fornari FA, Randolph JK, Yalowich JC, Ritke MK, and Gewirtz DA (1994). Interference by doxorubicin with DNA unwinding in MCF-7 breast tumor cells. *Mol Pharmacol.* **45**, 649-656.

(129) Rockwell S, Dobrucki IT, Kim EY, Marrison ST, and Vu VT (2009). Hypoxia and radiation therapy: past history, ongoing research, and future promise. *Curr Mol Med.* **9**, 442-458.

I

II

III

IV

Liposomal doxorubicin improves radiotherapy response in hypoxic prostate cancer xenografts

Eirik Hagtvet[1,2], Kathrine Røe[1,2,§], Dag Rune Olsen[3]

[1]Department of Radiation Biology, Institute for Cancer Research, The Norwegian Radium Hospital, Oslo University Hospital, P. O. Box 4953 Nydalen, 0424 Oslo, Norway

[2]Institute of Clinical Medicine, University of Oslo, Oslo, Norway

[3]Faculty of Mathematics and Natural Sciences, University of Bergen, Bergen, Norway

[§]Corresponding author

Email addresses:

EH: Eirik.Hagtvet@rr-research.no

[§]KR: Kathrine.Roe@rr-research.no

DRO: Dag.Olsen@mnfa.uib.no

Abstract

Background: Tumor vasculature frequently fails to supply sufficient levels of oxygen to tumor tissue resulting in radioresistant hypoxic tumors. To improve therapeutic outcome radiotherapy (RT) may be combined with cytotoxic agents.

Methods: In this study we have investigated the combination of RT with the cytotoxic agent doxorubicin (DXR) encapsulated in pegylated liposomes (PL-DXR). The PL-DXR formulation Caelyx® was administered to mice bearing prostate carcinoma xenografts, in combination with RT performed under normoxic and hypoxic conditions. Treatment response evaluation consisted of tumor volume measurements and dynamic contrast-enhanced magnetic resonance imaging (DCE MRI) with subsequent pharmacokinetic analysis using the Brix model. Imaging was performed pre-treatment (baseline) and 8 days later. Further, hypoxic fractions were determined by pimonidazole immunohistochemistry of excised tumor tissue.

Results: As expected, the therapeutic effect of RT was significantly less effective under hypoxic than normoxic conditions. However, concomitant administration of PL-DXR significantly improved the therapeutic outcome following RT in hypoxic tumors. Further, the pharmacokinetic DCE MRI parameters and hypoxic fractions suggest PL-DXR to induce growth-inhibitory effects without interfering with tumor vascular functions.

Conclusions: We found that DXR encapsulated in liposomes improved the therapeutic effect of RT under hypoxic conditions without affecting vascular functions. Thus, we propose that for cytotoxic agents affecting tumor vascular functions liposomes may be a promising drug delivery technology for use in chemoradiotherapy.

Background

During tumor growth abnormal tumor vasculature frequently fails to supply sufficient levels of oxygen to tumor tissue, resulting in various degrees of hypoxia [1,2]. Tumor hypoxia is known to cause treatment resistance and to promote metastatic disease progression [3-5]. To improve radiotherapy (RT) efficacy of radioresistant tumors, several approaches have been suggested [6,7]. One strategy is to combine conventional cytotoxic agents with RT to increase the therapeutic effects, i.e. chemoradiotherapy (CRT) [8,9].

The anthracycline chemotherapeutic drug doxorubicin (DXR) has been demonstrated to enhance the therapeutic effect of RT [10-13], presumably by preventing cells from repairing radiation-induced DNA damage [11-13]. DXR has also reportedly enhanced the effect of RT under experimental *in vitro* hypoxic conditions [14].

By encapsulating DXR in liposomes, DXR accumulation in the heart is reduced, resulting in less cardiac toxicities compared to conventional DXR [15,16]. Abnormal tumor vasculature also favors accumulation of liposomes due to the enhanced permeability retention effect [17]. Moreover, by incorporating polyethylene glycol (PEG) in the liposomal membrane, clearance by the cells of the reticulo-endothelial system is reduced, resulting in prolonged circulation time [18].

Liposomes accumulated in the tumor may act as depots for sustainable drug release, making them particularly beneficial during a course of CRT, since daily drug dosing would be needless [19]. Also, as liposomes avoid accumulation in healthy tissue, radiation enhancement may primarily be located to tumors, reducing toxicities in neighboring healthy tissues [19,20]. Pegylated liposomal DXR (PL-DXR) has been shown to increase the effect of RT in

preclinical studies [19,21] and promising results are also achieved in clinical applications [20,22].

The objective of this study was to evaluate the potential therapeutic benefit of administering PL-DXR (Caelyx®) to tumor-bearing mice receiving RT under hypoxic, radioresistant conditions. Therapy-mediated changes in tumor vascular functions and tumor hypoxia were assessed by dynamic contrast-enhanced magnetic resonance imaging (DCE MRI) and pimonidazole immunohistochemistry, respectively.

Methods

Materials

The PL-DXR product Caelyx® was supplied by the pharmacy at the Norwegian Radium Hospital, Oslo, Norway (European distributor; Schering-Plough). Pimonidazole hydrochloride was supplied by Natural Pharmacia International, Inc., Burlington, MA, USA, and the contrast agent Dotarem® was from Laboratoire Guerbet, Paris, France. Dako EnVision™+ System-HRP (DAB) was supplied by Dako Corporation, DA, USA.

For anaesthesia of mice a mixture of 2.4 mg/ml tiletamine and 2.4 mg/ml zolazepam (Zoletil® vet, Virbac Laboratories, Carros, France), 3.8 mg/ml xylazine (Narcoxyl® vet, Roche, Basel, Switzerland) and 0.1 mg/ml butorphanol (Torbugesic®, Fort Dodge Laboratories, Fort Dodge, IA, USA) was prepared and used.

Experimental animals

Male athymic nude Balb/c mice were provided by the Department of Comparative Medicine (animal facility), Oslo University Hospital. The CWR22 xenograft model, originating from a human, primary prostate carcinoma [23], was serially transplanted between mice. In brief, by blunt dissection through a skin incision tumor fragments (~2x2x2) mm^3 were subcutaneously implanted on the upper leg (proximal to the knee joint) of 4 - 5 weeks old mice. The skin incision was sealed with topical skin adhesive. Approximately three weeks later a tumor xenograft of 5 - 10 mm in diameter developed. The mice were housed in transparent boxes with bedding material, fed *ad libitum* and kept under specific pathogen-free conditions. The temperature and relative humidity were kept constant at 20 - 21°C and 60 %, respectively. At the end of the experiments all animals were euthanized by cervical dislocation. All procedures were performed according to protocols approved by the National Animal Research Authority

and carried out in compliance with the European Convention for the Protection of Vertebrates Used for Scientific Purposes.

Radiotherapy

RT was delivered at a dose of 2 Gy/day for five consecutive days (at experiment days 1 – 5) using a ^{60}Co source (Mobaltron 80, TEM instruments, Crawley, UK) with a dose rate of 0.8 Gy/min. The animals were located in a custom designed vicryl tube with an opening for the tumor bearing leg to be stretched out and fixated horizontally. During the procedure only the tumor bearing leg was extended into the radiation field, limiting radiation exposure to the remaining body. The procedure was performed under sedation induced by 0.05 ml of anesthetic agent.

Hypoxic radiotherapy

Tumor hypoxia was experimentally induced by placing the animals in a vicryl tube. A rubber band was clamped around the leg of the animal, proximal to the xenograft. The rubber band was left on for five minutes prior to and during RT (at experiment days 1 – 5). During clamping the animal's leg temporary turned bluish, indicating stagnation of blood circulation with concurrent induction of acute hypoxia. The discoloration disappeared rapidly following removal of the rubber band and no animals became lame or experienced any adverse effects from the clamping. The procedure was performed under sedation induced by 0.05 ml of anesthetic agent.

PL-DXR

PL-DXR was administered at a dose of 3.5 mg DXR/kg as a single i.v. bolus injection through the tail vein (at experiment day 0). The rationale for using the relatively low drug

dose was to avoid reaching therapy saturation levels where any additional effect produced by hypoxic RT would not be detected.

Monitoring of treatment response

Animals bearing tumor xenografts sized 5 - 10 mm in diameter were randomly allocated into different experimental groups of 8 - 10 tumors each (Table 1). At the start of the experiment all animals were imaged by DCE MRI with subsequent i.v. administration of PL-DXR to animals designated to the PL-DXR groups. RT treatment began 24 hrs later, enabling sufficient time for liposomal tumor accumulation. During daily RT sessions all animals, regardless of experimental group, were sedated. To assess therapy-induced changes in tumor vascular function all animals were subjected to an identical imaging protocol 8 days after the pre-treatment DCE MRI.

Tumor volumes were estimated after measuring the tumors' shortest and longest diameters with four days intervals using a digital caliper (Model B220S, Kroeplin, Schlüchtern, Germany). The tumor volume was calculated according to the formula $(\pi/6)*length^2*width$ [24].

DCE MRI acquisitions

MRI acquisitions were performed as previously described [25], using a 1.5 T GE Signa LS scanner (GE Medical Systems, Milwaukee, WI), and a dedicated MRI mouse coil [26]. Prior to MRI, a heparinized 24 G catheter attached to a cannula containing 0.01 ml/g body weight contrast agent (Dotarem®, diluted in heparinized saline to 0.06 M) was inserted into the animals' tail vein. The animals were placed in an adapted cradle and put into the coil, before being placed in the scanner. During image acquisition, the animal's temperature was maintained at 38 °C. First, the tumor was localized using axial fast spin-echo (FSE) T2-

weighted (T2W) images (echo time (TE_{eff}) = 85 ms, repetition time (TR) = 4000 ms, echo train length (ETL) = 16, image matrix (IM) = 256 × 256, field-of-view (FOV) = 4 cm, slice thickness (ST) = 2 mm). Second, DCE MRI was obtained with a dynamic fast spoiled gradient-recalled (FSPGR) T1W sequence (TE = 3.5 ms, TR = 180 ms, IM = 256 × 128, FOV = 6 cm, ST = 2 mm, and flip angle (FA) = 80°). Following 5 baseline T1W image acquisitions, contrast kinetics were investigated by injecting the contrast agent during 3 seconds and performing 20 minutes of post-contrast imaging. The time resolution was 12 seconds and the reconstructed voxel size was 0.23 × 0.23× 2 mm^3.

DCE MRI analysis

Image analysis was performed using in-house developed software in IDL (Interactive Data Language v 6.2, Research Systems Inc., Boulder, CO). For the central slice of each tumor, a region of interest (ROI) was manually traced in T1W images, excluding surrounding skin and connective tissue. The time-dependent relative signal intensity, *RSI(t)*, was calculated for each image voxel according to Equation 1.

Equation 1: $$RSI(t) = \frac{SI(t) - SI(0)}{SI(0)}$$

where *SI(0)* refers to the pre-contrast signal intensity and *SI(t)* the post-contrast signal intensity in the voxel at time *t*. Pharmacokinetic modeling was performed using the Brix model [27], with the *RSI(t)* for each voxel as input. The Brix model is a two-compartment pharmacokinetic model where the contrast agent is assumed to distribute between two individually well-mixed compartments; the blood plasma and the extracellular extravascular space (EES) in the tumor. The i.v. injected contrast agent is transported into the tumor by

perfusion, where it diffuses between the plasma and the EES, before being eliminated at a constant rate.

Using the *RSI(t)* for each voxel in the tumor ROI, the Brix model (equation 2) was fitted using the Levenberg-Marquardt least-squares minimization method (MPFIT; http://purl.com/net/mpfit) [28].

Equation 2: $$RSI(t) = \frac{Ak_{ep}}{k_{el}k_{ep}}(e^{-k_{ep}t} - e^{-k_{el}t})$$

where the parameter k_{ep} is the rate constant between plasma and EES, k_{el} the clearance rate of contrast agent from plasma, and A an amplitude parameter related to the size of the EES.

Immunohistochemistry of tumor hypoxia

In addition to the animals subjected to DCE MRI, parallel groups of animals were followed to harvest tumor tissue at the same time-point as the day 8 MRI acquisitions. Animals designated to immunohistochemistry examination received identical treatments as animals used for tumor growth assessment and DCE MRI (Table 1), with each group containing 8 tumors. Hypoxia was determined by injecting 80 mg/kg pimonidazole hydrochloride (1-[(2-hydroxy-3-piperidinyl)propyl]-2-nitroimidazole hydrochloride, dissolved in saline i.p. One hour later euthanasia was performed by cervical dislocation and tumors were excised and preserved in phosphate-buffered 4 % formalin until tissue sectioning. Tumor hypoxia was detected using a peroxidase-based immunostaining method. In brief, tissue sections were stained using the Dako EnVision™+ System-HRP (DAB) (K4011) and Dakoautostainer. Deparaffinization and unmasking of epitopes were performed using PT-Link (DAKO) and EnVision™ Flex target retrieval solution, high pH. To block endogenous peroxidase, sections were treated with 0.03

% hydrogen peroxide for 5 minutes. The preparations were incubated 30 minutes with polyclonal rabbit antibodies to pimonidazole-protein adducts (1:10000 dilution). The sections were then incubated with peroxidase-labeled polymer conjugated to goat anti-rabbit secondary antibodies for 30 minutes. The tissue sections were stained for 10 minutes with 3'3-diaminobenzidine tetrachloride (DAB) and counterstained with haematoxylin, dehydrated and mounted in Diatex.

Statistical analysis

By means of a multiple regression procedure differences in tumor growth between the experimental groups were operationally represented by three between group comparisons; 1) comparing the RT group with the hypoxic RT group, 2) comparing the RT group with the PL-DXR group and finally, 3) comparing the hypoxic RT group with the PL-DXR + hypoxic RT group. Tumor growth was represented by linear and quadratic developmental trends.

Group differences in DCE MRI parameters and hypoxic fractions were analyzed by student's *t*-tests, and the Pearson correlation (*r*) test analyzed whether correlations between variables were significant using SPSS 16.0 (SPSS, Cary, NC). A significance level of 5 % was used for all statistical analyses.

Results

Tumor growth

Tumor volume measurements were performed with four days intervals for 29 days, except for the control group where animals were euthanized at day 21 when the tumor diameters exceeded 20 mm, i.e. in accordance with internal regulations for animal experiments. Based on the 21 days observation period, the tumor growth of the control group was significantly enhanced as compared to all the groups receiving treatment ($p<0.050$). The differences in tumor growth between the remaining groups were analyzed on the basis of the 29 days observation period. Based on quadratic developmental trends the hypoxic RT group showed significantly less therapeutic effect than the normoxic RT group (comparison 1, $p=0.006$). The group receiving PL-DXR also presented significantly less therapeutic effect than the RT group (comparison 2, $p=0.008$). Interestingly, tumor growth in the PL-DXR + hypoxic RT group was significantly reduced compared to the hypoxic RT group (comparison 3, $p=0.004$). Tumor growth patterns are portrayed in Figure 1. No adverse effects were observed in any of the experimental groups.

Treatment monitoring using DCE MRI

Following Brix modeling of contrast kinetics, parametric images of A, k_{el} and k_{ep} were produced. The k_{ep} parameter is a parameter mainly related to the in-wash of contrast agent from plasma to extravascular space. Due to a very rapid contrast agent in-wash, presumably caused by high permeability and/or high perfusion, some tumor voxels were saturated, precluding estimation of reliable mean tumor values of k_{ep} for subsequent intergroup comparisons. The k_{ep} parameters were therefore excluded. Also, due to unsuccessful injection of contrast agent or technically related issues, some of the tumors in the experiment were excluded from subsequent pharmacokinetic analysis. Further, some of the tumors were too

small to enable reliable DCE MRI analysis. The exact number of tumors that underwent MRI and image analysis is indicated in all relevant figures onwards.

In Figure 2, the mean group relative change in the *A* parameter from day 0 to day 8 is presented. A reduction in the *A* parameter was observed for both the control (18 %) and the PL-DXR (26 %, p=0.030) groups. All groups receiving radiation experienced a relative increase from day 0 to day 8, being 4 % in the PL-DXR + hypoxic RT group, 20 % (p=0.002) in the hypoxic RT group and 29 % (p=0.046) in the RT group. No significant intergroup difference in the *A* parameter was observed when comparing the control tumors with tumors treated with PL-DXR. However, all groups receiving radiation experienced a significant increase in the *A* parameter compared to the control group; PL-DXR + hypoxic RT (p=0.019), hypoxic RT (p=0.001) and RT (p=0.006). Additionally, the group receiving PL-DXR + hypoxic RT also experienced an increase in the *A* parameter compared to PL-DXR (p=0.026) and a decrease compared to hypoxic RT (p=0.025) and RT (p=0.049).

In Figure 3, the mean group relative change in the k_{el} parameter from day 0 to day 8 is presented. Three groups experienced an increase in k_{el}, being 45 % in the control group, 85 % in the PL-DXR group and 47 % in the PL-DXR + hypoxic RT group. Due to large intragroup variations, these increases were not significant. Both the hypoxic and normoxic RT groups experienced a 27 % decrease in the k_{el} parameter with the change in the hypoxic RT group being significant (p=0.007). No intergroup differences in the k_{el} parameter were observed when comparing the control tumors with the tumors that received PL-DXR or PL-DXR + hypoxic RT. However, both the hypoxic RT group and the RT group experienced significant reductions in the k_{el} parameter compared to the control group, (p=0.015 and p=0.020, respectively).

Immunohistochemistry of tumor hypoxia

Parallel to tumor growth and DCE MRI studies identically treated groups of tumors were excised and used to assess tumor hypoxia at day 8, coinciding with the time-point of post-treatment MRI acquisitions. Figure 4 presents the hypoxic fractions of the different experimental groups. The mean hypoxic fractions were 23 % for the control tumors, 21 % for tumors treated with PL-DXR alone, 14 % for the tumors receiving both PL-DXR and hypoxic RT, 15 % for tumors receiving hypoxic RT, and 11 % for tumors receiving RT. Compared to the control group, only the RT group presented significantly reduced hypoxic fractions (p=0.041).

Correlations

Figure 5 shows the correlations between the mean group hypoxic fractions at day 8 (%) versus the mean group relative change in the *A* parameter from day 0 to day 8 (%) (Figure 5A), the mean group relative change in the k_{el} parameter from day 0 to day 8 (%) (Figure 5B), and the mean group relative change in tumor volumes from day 0 to day 9 (%) (Figure 5C), respectively. The mean group hypoxic fractions showed a strong negative correlation to the mean group relative change in the *A* parameter from day 0 to day 8 (r=-0.93, p=0.022), a weaker and insignificant positive correlation to the mean group relative change in the k_{el} parameter from day 0 to day 8 (r =0.74, p=0.155), and a positive correlation to the mean group tumor volume change from day 0 to day 9 (r=0.94, p=0.019).

Figure 6 shows the correlations between the mean group relative change in tumor volumes from day 0 to day 9 (%) versus the mean group relative change in the *A* parameter from day 0 to day 8 (%) (Figure 6A) and the mean group relative change in the k_{el} parameter from day 0 to day 8 (%) (Figure 6B), respectively. Mean group tumor volume change correlated negatively to the mean group relative change in the *A* parameter (r=-0.91, p=0.030) from day

0 to day 8, and positively, but not significantly, to the mean group relative change in the k_{el} parameter (r=0.75).

Discussion

Tumor hypoxia prevent effective RT [3-5], and several strategies to improve RT efficacy under hypoxic conditions have been described [6,7]. The ability of PL-DXR to enhance the therapeutic effect of fractionated and single dose RT has previously been reported [19,21]. In the current study we demonstrated that PL-DXR improves the therapeutic effect of RT also under hypoxic conditions. Moreover, as it is important to develop strategies to monitor treatment responses non-invasively, DCE MRI appears to be promising for this purpose.

The current PL-DXR formulation accumulates slowly in tumors, reaching peak levels 2-3 days post injection in tumor xenograft models [29,30]. Consequently, substantial levels of PL-DXR in the tumors during the five days of RT were expected. Any RT-mediated changes in tumor vascular functions that could interfere with tumor liposome accumulation was expected to be minimal as RT previously has reported to not alter liposomal tumor uptake [31,32].

Free DXR is reported to decrease tumor blood flow [33,34], subsequently reducing the oxygen levels in tumors. In contrary, PL-DXR has been suggested to normalize tumor vasculature [35]. In the current study there was no significant difference between the control and the PL-DXR group in any of the DCE MRI derived kinetic parameters or hypoxic fractions, suggesting that PL-DXR did not alter vascular functions. Still, tumor growth was significantly inhibited indicating that PL-DXR may exert tumoricidal effects without interfering with tumor blood circulation. This feature is highly beneficial with respect to subsequent RT since well oxygenated and vascularized tumors more likely respond better to RT.

In contrary, RT induced changes in the tumor vasculature both in the hypoxic and normoxic tumors, as measured by an increase in the *A* parameter. This alternation may be related to an increased interstitial volume, and a reduced elimination rate of contrast agent, as indicated by the k_{el} parameter. The increase seen in the *A* parameter may be related to radiation-induced necrosis and/or edema, and thus increased interstitial volume. Further, an increase in the *A* parameter may reflect disrupted membranes increasing the extracellular volume due to elevated membrane permeability. Finally, the observed reductions in the k_{el} parameter may reflect radiation-induced endothelial cell death, making clearance of contrast agent less effective. Interestingly, when hypoxic RT was administered in combination with PL-DXR these changes became less evident, indicating that PL-DXR reduced some of the vascular effects caused by RT in hypoxic tumors.

Figure 5A shows that the hypoxic fractions were significantly correlated to the changes in the *A* parameter from day 0 to day 8. A similar relation has also been found in a clinical DCE MRI study of cervical cancer, where a positive correlation between the *A* parameter and oxygen levels, as measured by Eppendorf pO_2 histography, was evidenced [36]. This may suggest the *A* parameter as a candidate biomarker of tumor hypoxia, for further investigation. The k_{el} parameter correlated less to hypoxia, as seen in Figure 5B. Moreover, hypoxic fractions correlated significantly (Figure 5C) with tumor volume changes and may explain why the measured hypoxic fractions were highest in the control tumors and lowest in the tumors receiving the most effective treatments. Hypoxia and tumor size have also previously been demonstrated to correlate strongly [37].

The treatment-induced changes in the *A* parameter correlated significantly and negatively to tumor volume changes (Figure 6A), and changes in the k_{el} parameter correlated strongly and

positively, although not significantly, to these volume changes (Figure 6B). This is promising with respect to developing DCE MRI and pharmacokinetic image analysis as tools for non-invasive monitoring of therapeutic effects.

The presence of oxygen in tumors exposed to RT is crucial because oxygen 1) enhance the yield of radiation-induced radicals and thus DNA damage, and 2) prevent repair of induced DNA damage by fixation of the damage [38]. DXR enhances the therapeutic effect of RT presumably by preventing cells from repairing radiation-induced DNA damage [11-13]. DXR may therefore resemble the effect of oxygen in tumors exposed to RT. Hypoxia is a common feature amongst most clinical tumors [39]. Overcoming hypoxia by administration of radiosensitizing drugs may nevertheless be of limited success as supply to hypoxic regions commonly are hampered by inadequate vascularization. Liposomal DXR seems however to have a positive effect on the tumor vascular functions as shown in this study.

Conclusion

The present study shows that PL-DXR improves the therapeutic effect of RT under hypoxic conditions and that PL-DXR does not affect tumor vascular functions. Interestingly, PL-DXR appeared to reduce some of the vascular alterations induced in hypoxic tumors by RT. Hence, for drugs that affect tumor vascular functions liposomes may be a promising drug delivery technology for use in CRT.

Competing interests

The authors report no competing interests.

Authors' contributions

EH participated in study design, carried out the animal experiments, MRI data acquisition, immunohistochemistry analysis and wrote the manuscript. KR participated in study design, analyzed the MRI data and contributed to data discussion and revision of the manuscript. DRO participated in study design, data discussion and revision of the manuscript. All authors read and approved the final manuscript.

Acknowledgements

The authors would like to thank Professor F. Saatcioglu, University of Oslo, for providing the CWR22 xenograft, Professor Knut Hagtvet, University of Oslo for valuable advice regarding the statistical analysis of tumor growth patterns and Tord Hompland, Department of Radiation Biology, Institute for Cancer Research, Oslo University Hospital, for contributing with his MRI expertise.

The project was supported by the Norwegian Research Council (NANOMAT programme, to EH), the South-Eastern Norway Regional Health Authority (grant 2009070, to KR) and the European Union 7th Framework Programme Grant 222741 – METOXIA.

References

1. Hockel M, Vaupel P: **Tumor hypoxia: definitions and current clinical, biologic, and molecular aspects.** *J Natl Cancer Inst* 2001, **93**:266-276.

2. Vaupel P, Kelleher DK, Hockel M: **Oxygen status of malignant tumors: pathogenesis of hypoxia and significance for tumor therapy.** *Semin Oncol* 2001, **28**:29-35.

3. Marignol L, Coffey M, Lawler M, Hollywood D: **Hypoxia in prostate cancer: a powerful shield against tumour destruction?** *Cancer Treat Rev* 2008, **34:**313-327.

4. Rudolfsson SH, Bergh A: **Hypoxia drives prostate tumour progression and impairs the effectiveness of therapy, but can also promote cell death and serve as a therapeutic target.** *Expert Opin Ther Targets* 2009, **13**:219-225.

5. Stewart GD, Ross JA, McLaren DB, Parker CC, Habib FK, Riddick AC: **The relevance of a hypoxic tumour microenvironment in prostate cancer.** *BJU Int* 2010, **105**:8-13.

6. Overgaard J: **Hypoxic radiosensitization: adored and ignored.** *J Clin Oncol* 2007, **25**:4066-4074.

7. Wouters BG, Weppler SA, Koritzinsky M, Landuyt W, Nuyts S, Theys J, Chiu RK, Lambin P: **Hypoxia as a target for combined modality treatments.** *Eur J Cancer* 2002, **38**:240-257.

8. Bentzen SM, Harari PM, Bernier J: **Exploitable mechanisms for combining drugs with radiation: concepts, achievements and future directions.** *Nat Clin Pract Oncol* 2007, **4**:172-180.

9. Seiwert TY, Salama JK, Vokes EE: **The concurrent chemoradiation paradigm--general principles.** *Nat Clin Pract Oncol* 2007, **4**:86-100.

10. Bellamy AS, Hill BT: **Interactions between clinically effective antitumor drugs and radiation in experimental systems.** *Biochim Biophys Acta* 1984, **738**:125-166.

11. Bonner JA, Lawrence TS: **Doxorubicin decreases the repair of radiation-induced DNA damage.** *Int J Radiat Biol* 1990, **57**:55-64.

12. Byfield JE, Lynch M, Kulhanian F, Chan PY: **Cellular effects of combined adriamycin and x-irradiation in human tumor cells.** *Int J Cancer* 1977, **19**:194-204.

13. Watring WG, Byfield JE, Lagasse LD, Lee YD, Juillard G, Jacobs M, Smith ML: **Combination Adriamycin and radiation therapy in gynecologic cancers.** *Gynecol Oncol* 1974, **2**:518-526.

14. Durand RE: **Adriamycin: a possible indirect radiosensitizer of hypoxic tumor cells.** *Radiology* 1976, **119**:217-222.

15. Batist G: **Cardiac safety of liposomal anthracyclines.** *Cardiovasc Toxicol* 2007, **7:**72-74.

16. Ewer MS, Martin FJ, Henderson C, Shapiro CL, Benjamin RS, Gabizon AA: **Cardiac safety of liposomal anthracyclines.** *Semin Oncol* 2004, **31**:161-181.

17. Maeda H, Wu J, Sawa T, Matsumura Y, Hori K: **Tumor vascular permeability and the EPR effect in macromolecular therapeutics: a review.** *J Control Release* 2000, **65**:271-284.

18. Gabizon A, Shmeeda H, Barenholz Y: **Pharmacokinetics of pegylated liposomal Doxorubicin: review of animal and human studies.** *Clin Pharmacokinet* 2003, **42**:419-436.

19. Harrington KJ, Rowlinson-Busza G, Syrigos KN, Vile RG, Uster PS, Peters AM, Stewart JS: **Pegylated liposome-encapsulated doxorubicin and cisplatin enhance the effect of radiotherapy in a tumor xenograft model.** *Clin Cancer Res* 2000, **6**:4939-4949.

20. Koukourakis MI, Koukouraki S, Giatromanolaki A, Kakolyris S, Georgoulias V, Velidaki A, Archimandritis S, Karkavitsas NN: **High intratumoral accumulation of stealth liposomal doxorubicin in sarcomas--rationale for combination with radiotherapy.** *Acta Oncol* 2000, **39:**207-211.

21. Davies CL, Lundstrom LM, Frengen J, Eikenes L, Bruland S OS, Kaalhus O, Hjelstuen MH, Brekken C: **Radiation improves the distribution and uptake of liposomal doxorubicin (caelyx) in human osteosarcoma xenografts.** *Cancer Res* 2004, **64**:547-553.

22. Koukourakis MI, Koukouraki S, Giatromanolaki A, Archimandritis SC, Skarlatos J, Beroukas K, Bizakis JG, Retalis G, Karkavitsas N, Helidonis ES: **Liposomal doxorubicin and conventionally fractionated radiotherapy in the treatment of locally advanced non-small-cell lung cancer and head and neck cancer.** *J Clin Oncol* 1999, **17**:3512-3521.

23. Pretlow TG, Wolman SR, Micale MA, Pelley RJ, Kursh ED, Resnick MI, Bodner DR, Jacobberger JW, Delmoro CM, Giaconia JM, Pretlow TP: **Xenografts of primary human prostatic carcinoma.** *J Natl Cancer Inst* 1993, **85**:394-398.

24. Favier J, Lapointe S, Maliba R, Sirois MG: **HIF2 alpha reduces growth rate but promotes angiogenesis in a mouse model of neuroblastoma.** *BMC Cancer* 2007, **7**:139.

25. Roe K, Seierstad T, Kristian A, Mikalsen LT, Maelandsmo GM, van der Kogel AJ, Ree AH, Olsen DR: **Longitudinal magnetic resonance imaging-based assessment of vascular changes and radiation response in androgen-sensitive prostate carcinoma xenografts under androgen-exposed and androgen-deprived conditions.** *Neoplasia* 2010, **12**:818-825.

26. Seierstad T, Roe K, Hovik B: **Construction of a modified capacitive overlap MR coil for imaging of small animals and objects in a clinical whole-body scanner.** *Phys Med Biol* 2007, **52**:N513-N522.

27. Brix G, Semmler W, Port R, Schad LR, Layer G, Lorenz WJ: **Pharmacokinetic parameters in CNS Gd-DTPA enhanced MR imaging.** *J Comput Assist Tomogr* 1991, **15**:621-628.

28. Markwardt CB: **Non-Linear Least Squares Fitting in IDL with MPFIT.** *proc Astronomical Data Analysis Software and Systems XVIII, Quebec, Canada, ASP Conference Series.* 2008, **411**:251-254.

29. Gabizon A, Tzemach D, Mak L, Bronstein M, Horowitz AT: **Dose dependency of pharmacokinetics and therapeutic efficacy of pegylated liposomal doxorubicin (DOXIL) in murine models.** *J Drug Target* 2002, **10**:539-548.

30. Gabizon A, Goren D, Horowitz AT, Tzemach D, Lossos A, Siegal T: **Long-circulating liposomes for drug delivery in cancer therapy: a review of**

biodistribution studies in tumor-bearing animals. *Adv Drug Deliver Rev* 1997, **24**:337-344.

31. Harrington KJ, Rowlinson-Busza G, Uster PS, Vile RG, Peters AM, Stewart JS: **Single-fraction irradiation has no effect on uptake of radiolabeled pegylated liposomes in a tumor xenograft model.** *Int J Radiat Oncol Biol Phys* 2001, **49**:1141-1148.

32. Harrington KJ, Rowlinson-Busza G, Syrigos KN, Uster PS, Vile RG, Peters AM, Stewart JS: **The effect of irradiation on the biodistribution of radiolabeled pegylated liposomes.** *Int J Radiat Oncol Biol Phys* 2001, **50**:809-820.

33. Durand RE, LePard NE: **Modulation of tumor hypoxia by conventional chemotherapeutic agents.** *Int J Radiat Oncol Biol Phys* 1994, **29**:481-486.

34. Durand RE, LePard NE: **Tumour blood flow influences combined radiation and doxorubicin treatments.** *Radiother Oncol* 1997, **42**:171-179.

35. Verreault M, Strutt D, Masin D, Anantha M, Yung A, Kozlowski P, Waterhouse D, Bally MB, Yapp DT: **Vascular normalization in orthotopic glioblastoma following intravenous treatment with lipid-based nanoparticulate formulations of irinotecan (Irinophore C), doxorubicin (Caelyx(R)) or vincristine.** *BMC Cancer* 2011, **11**:124.

36. Loncaster JA, Carrington BM, Sykes JR, Jones AP, Todd SM, Cooper R, Buckley DL, Davidson SE, Logue JP, Hunter RD, West CM: **Prediction of radiotherapy outcome using dynamic contrast enhanced MRI of carcinoma of the cervix.** *Int J Radiat Oncol Biol Phys* 2002, **54**:759-767.

37. Saitoh J, Sakurai H, Suzuki Y, Muramatsu H, Ishikawa H, Kitamoto Y, Akimoto T, Hasegawa M, Mitsuhashi N, Nakano T: **Correlations between in vivo tumor weight, oxygen pressure, 31P NMR spectroscopy, hypoxic microenvironment marking by beta-D-iodinated azomycin galactopyranoside (beta-D-IAZGP), and radiation sensitivity.** *Int J Radiat Oncol Biol Phys* 2002, **54**:903-909.

38. Bussink J, Kaanders JH, van der Graaf WT, Oyen WJ: **PET-CT for radiotherapy treatment planning and response monitoring in solid tumors.** *Nat Rev Clin Oncol* 2011, **8**:233-242.

39. Rockwell S, Dobrucki IT, Kim EY, Marrison ST, Vu VT: **Hypoxia and radiation therapy: past history, ongoing research, and future promise.** *Curr Mol Med* 2009, **9**:442-458.

Figures

Figure 1 – Tumor growth patterns for the experimental groups

Presented as mean ± SEM (n = 8 – 10 per group). The control group was removed from the study at day 21 due to tumor diameters exceeding 20 mm.

Figure 2 – Relative change in the *A* parameter (mean ± SEM) from day 0 to day 8 for the experimental groups

3.5 mg/kg PL-DXR was administered after pre-treatment DCE MRI. RT was delivered at a dose of 2 Gy/day for 5 consecutive days, starting 24 hours after the pre-treatment DCE MRI. Hypoxia was induced by clamping the tumor-bearing leg 5 minutes prior to and during RT. Significant differences ($p<0.050$) to the control or PL-DXR + hypoxic RT groups are indicated with # or ×, respectively.

Figure 3 – Relative change in the k_{el} parameter (mean ± SEM) from day 0 to day 8 for the experimental groups

3.5 mg/kg PL-DXR was administered after pre-treatment DCE MRI. RT was delivered at a dose of 2 Gy/day for 5 consecutive days, starting 24 hours after pre-treatment DCE MRI. Hypoxia was induced by clamping the tumor-bearing leg 5 minutes prior to and during RT. Significant differences ($p<0.050$) to the control or PL-DXR + hypoxic RT groups are indicated with # or ×, respectively.

Figure 4 – Hypoxic fractions in the experimental groups at day 8 assessed from pimonidazole immunohistochemistry of tumor tissue sections

Group mean and SEM are shown, with n = 8 per group. 3.5 mg/kg PL-DXR was administered 24 hours prior to RT. RT was delivered at a dose of 2 Gy/day for 5 consecutive days. Hypoxia

was induced by clamping the tumor-bearing leg 5 minutes prior to and during RT. A significant difference ($p<0.05$) to the control group is indicated with #.

Figure 5 – Hypoxic fractions versus DCE MRI parameters and tumor volumes

Correlations between the mean group hypoxic fractions (%) at day 8 versus the mean group relative change in the *A* parameter from day 0 to day 8 (%) (A), the mean group relative change in the k_{el} parameter from day 0 to day 8 (%) (B), and the relative change in mean group tumor volumes from day 0 to day 9 (%) (C), respectively.

Figure 6 – Tumor volume changes versus DCE MRI parameter changes

Correlations between the mean group relative change in tumor volumes (%) from day 0 to day 9 (%) versus the mean group relative change in the *A* parameter from day 0 to day 8 (%) (A), and the mean group relative change in the k_{el} parameter from day 0 to day 8 (%) (B), respectively.

Table 1. Overview of treatments administered to the different experimental groups.

Experimental groups	**Treatment**
Control	No treatment
PL-DXR	3.5 mg DXR/kg (day 0)
PL-DXR + hypoxic RT	3.5 mg DXR/kg (day 0) + clamping + 2 Gy/day for 5 days (day 1 – day 5)
RT	2 Gy/day for 5 days (day 1 – day 5)
Hypoxic RT	Clamping + 2 Gy/day for 5 days (day 1 – day 5)

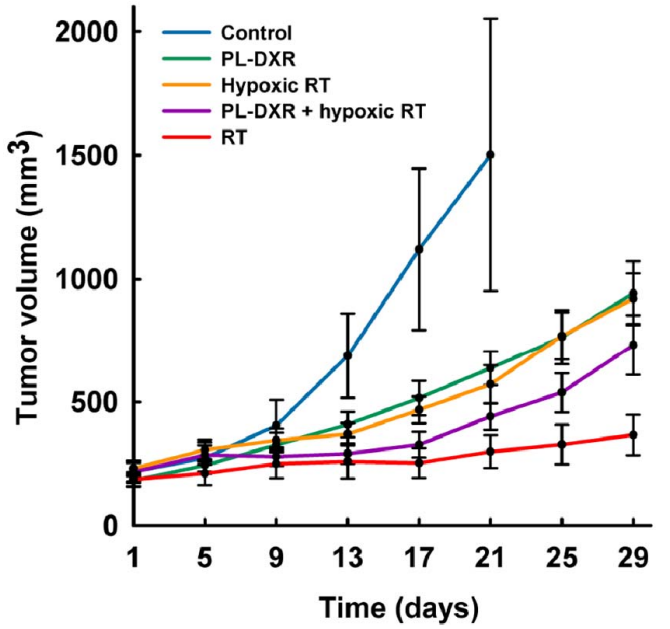

Figure 1.

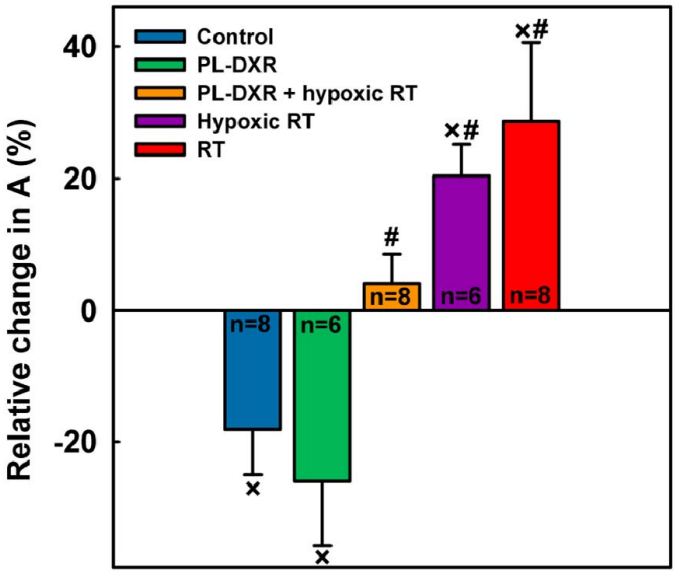

Figure 2.

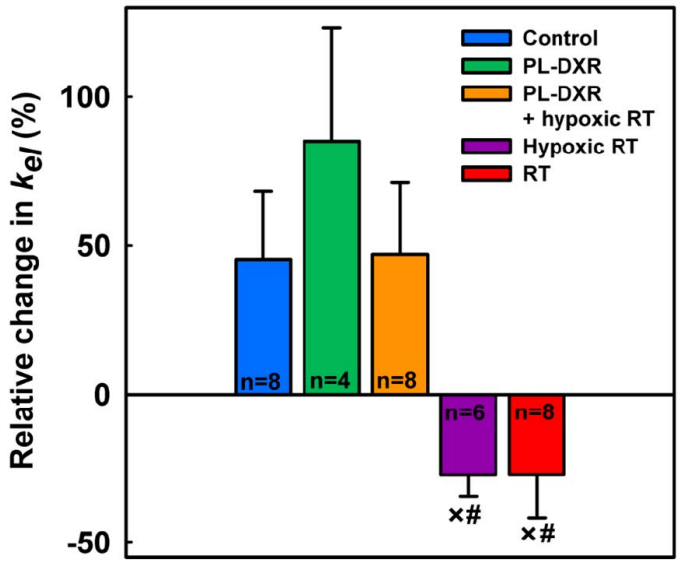

Figure 3.

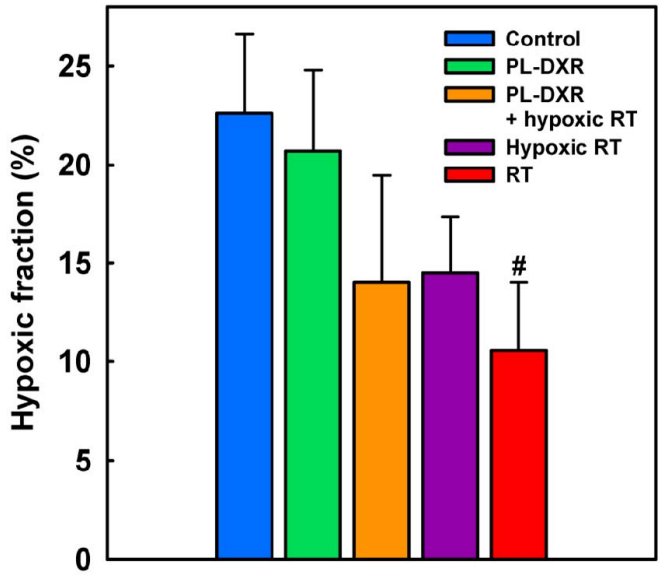

Figure 4.

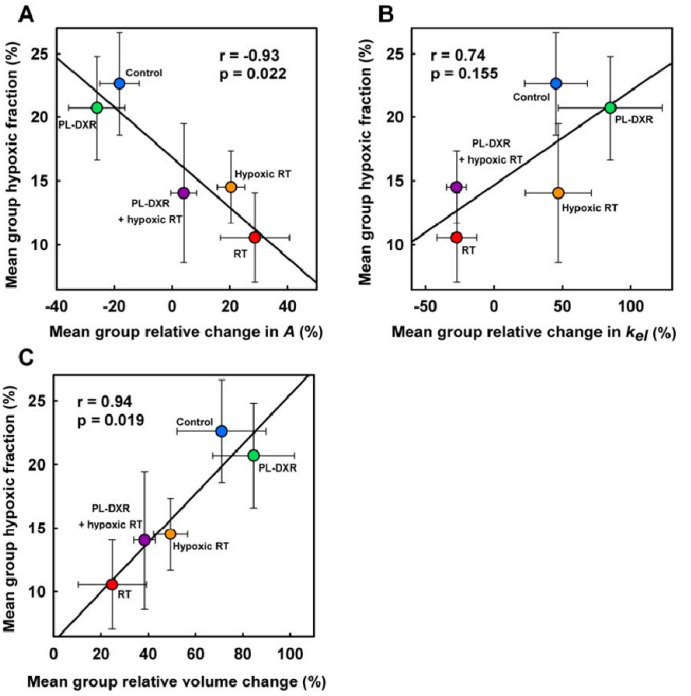

Figure 5.

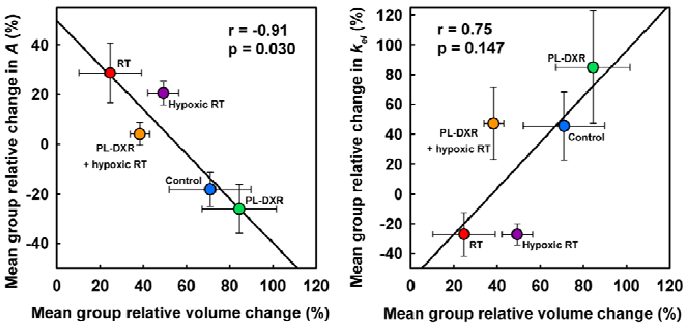

Figure 6.